Nano Research

Open Access

Review Article

Precision surface engineering of atomic scale metal nanocatalysts to enhance reaction activity and stability

Yuyao Sun, Zijing Suo, Jianping Lai ✉, and Lei Wang ✉

State Key Laboratory Base of Eco-Chemical Engineering, Ministry of Education, International Science and Technology Cooperation Base of Eco-chemical Engineering and Green Manufacturing, College of Chemistry and Molecular Engineering, Qingdao University of Science and Technology, Qingdao 266042, China

Cite this article: *Nano Research*, **2026**, *19*, 94908405. https://doi.org/10.26599/NR.2026.94908405

ABSTRACT: Atomic scale surface engineering of metal nanocatalysts is a key strategy for enhancing their catalytic performance. By precisely controlling the arrangement of surface atoms and their electronic structure, reaction activity, selectivity, and stability can be significantly improved. This review systematically summarizes recent advances in atomic level surface processing, including strategies, such as surface defect engineering, interface regulation, and dynamic encapsulation, and delves into their application mechanisms in fields like electrocatalysis and energy conversion. Nevertheless, challenges persist in this field, including synthetic controllability, tracking of dynamic structural evolution, precise design of active sites, and industrial-scale scaling. Future research must integrate multidisciplinary approaches, such as *in situ* characterization, theoretical simulations, and artificial intelligence, to advance the rational design and practical application of atomically precise catalysts, thereby providing novel insights for achieving highly efficient and stable energy conversion systems.

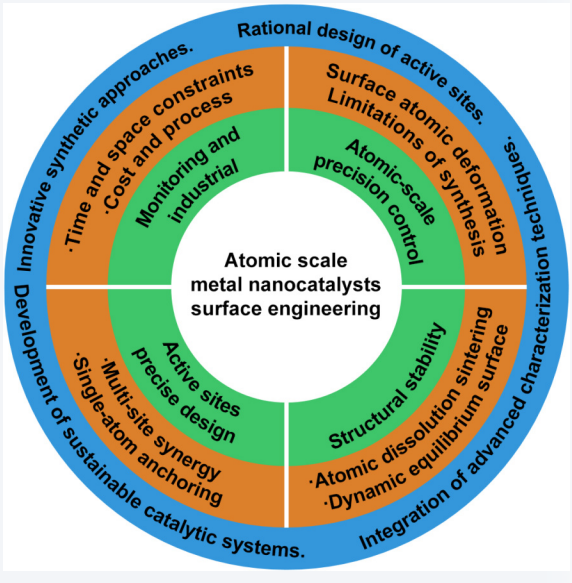

KEYWORDS: atomic processing, surface engineering, metal catalysts, nanoscale

1 Introduction

With the increasing depletion of fossil fuel resources and the growing prominence of environmental issues stemming from it, the development and utilization of renewable energy, along with the efficient conversion and storage of energy, have become key directions in scientific research and industrial applications [1–7]. Catalytic technology plays an irreplaceable role as a key enabler in energy conversion processes [8–15]. Catalysts significantly reduce reaction energy barriers, enhance reaction rates and selectivity, thereby improving energy utilization efficiency and minimizing byproduct and pollutant generation [16–19]. Researchers have consistently focused on understanding and optimizing catalyst active sites to achieve precise control over reaction pathways at the atomic scale [20–25]. In particular, metal nanoparticle catalysts exhibit outstanding performance in catalytic conversions due to their high specific surface area, tunable electronic structure, and abundant surface active sites [26–29]. Among these, the size, morphology, composition, and interface structure between metal particles and their supports profoundly influence catalytic activity and stability in applications, such as water electrolysis for hydrogen production, carbon dioxide reduction, and oxygen reduction reactions (ORRs) in fuel cells [30–35].

Nevertheless, metal nanocatalysts still face numerous challenges at the surface atom engineering level, which directly affect catalyst activity, selectivity, and stability [36–40]. Surface atomic engineering refers to the precise manipulation of catalyst surfaces at the atomic scale, encompassing atom-level synthesis, modification, arrangement, and defect engineering [41–46]. Research in this field is crucial for developing high-performance catalysts to meet future

Received: November 19, 2025; **Revised:** December 31, 2025
Accepted: January 5, 2026

✉Address correspondence to Jianping Lai, jplai@qust.edu.cn; Lei Wang, inorchemwl@126.com

energy and environmental demands [47–49]. In recent years, advancements in characterization techniques and computational methods have deepened scientists' understanding of surface atom engineering in metal nanocatalysts [50, 51]. Significant progress has been made, particularly in atomic level precision control, dynamic structural stability, active site design, and characterization technologies. However, these advances have not fully resolved key challenges at the surface atomic engineering level, leaving considerable gaps before achieving precise control over catalyst surface atoms. It is worth noting that although many relevant comprehensive reviews have been published in recent years, most only summarize synthesis strategies or characterization technologies, or vaguely define core concepts, lacking systematic analysis. This review takes the bottlenecks of atomic scale surface engineering as the core clue, connecting key links, such as synthesis controllability, dynamic stability, and industrial transformation. At the same time, it clearly distinguishes the core connotations and action mechanisms of defect engineering, interface regulation, and dynamic encapsulation. In addition, it strengthens interdisciplinary integration and practical orientation, not only integrating cutting edge technologies, such as artificial intelligence (AI) and synthetic biology, but also highlighting the need for green chemistry and industrial implementation.

Based on this, this review systematically reviews the latest research progress of surface atomic engineering of metal nanocatalysts, focuses on its key challenges, and outlines future development directions, providing references for research in this field.

2 Technical bottlenecks in atomic level precision control

2.1 Limitations in controllability of synthesis methods

Although techniques like atomic layer deposition (ALD) can achieve atomic level growth, precise control within complex carrier channels remains challenging [52]. Due to mass transfer resistance and interference from defect sites, metal atom distribution is often non-uniform. In conventional wet chemical etching or plasma etching processes, it is difficult to achieve precise removal at the single atom level [53]. The surface atomic electrochemical knock-out method developed by Qiu and co-workers [54] precisely removes Cu atoms from Cu_3Pd alloy catalysts through an electrically driven process, realizing quantitative removal of Cu atoms. Thus, it regulates materials at the atomic level, providing a new material synthesis and regulation method for wide applications in catalysis, energy, and other fields. This method uses electrochemical principles and through precise control of potential and time, can selectively remove metal atoms at specific locations to achieve precise regulation at the atomic level. However, the universality and cost effectiveness of this method still need further verification.

He and co-workers [55] successfully synthesized Ir@$SrIrO_3$ heterojunctions through a top to down partial dissolution strategy, and used them as efficient and stable acidic water splitting catalysts (Fig. 1(a)). Electrochemical performance test results showed that in 0.5 M H_2SO_4 solution, the overpotentials of Ir@$SrIrO_3$ catalysts for oxygen evolution reaction (OER) and hydrogen evolution reaction (HER) at a current density of 10 mA·cm^{-2} were 229 and 28 mV, respectively, and they showed excellent reaction stability. This method provides a new way for top to down preparation of metal ions with specific sizes, which is beneficial to the future design of size-controlled oxygen reduction electrocatalysts. However, the top-down partial dissolution strategy has strict requirements on the crystal structure and surface properties of the support. It is only suitable for specific perovskite structured supports. The bonding strength of the heterojunction interface depends on the precise control of dissolution conditions. Once the process parameters fluctuate, it is easy to cause the peeling of Ir nanoparticles from the $SrIrO_3$ support. Moreover, Sr precursors are expensive, lack low-cost alternative solutions, and their large-scale application is limited.

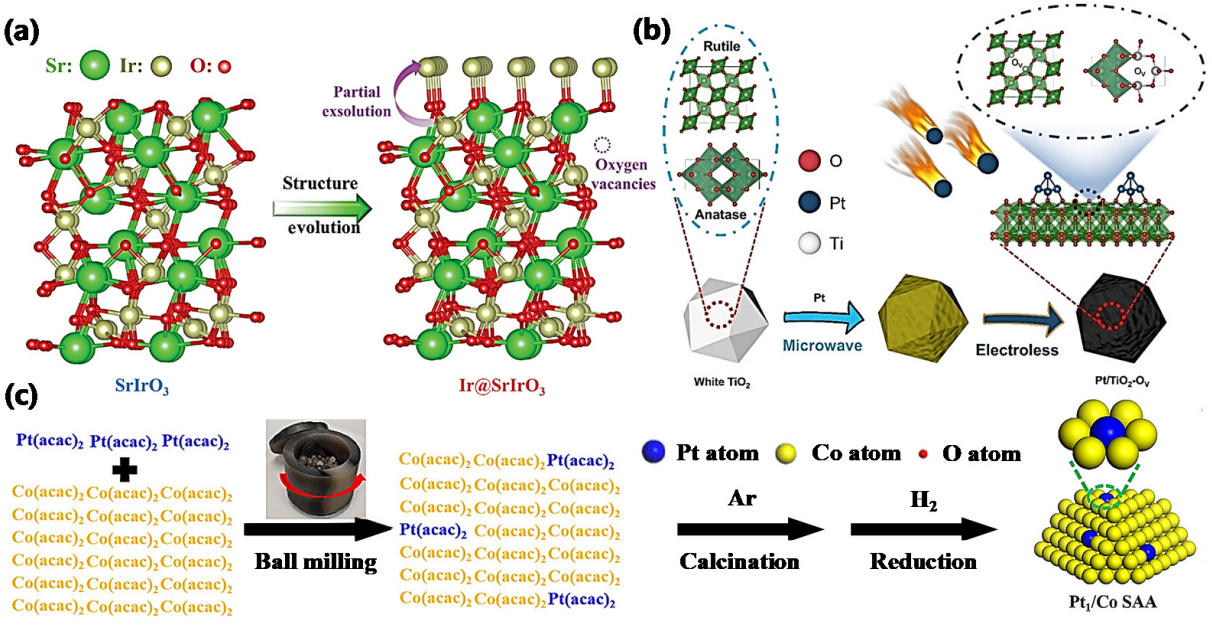

Figure 1 (a) Schematic diagram of the structural evolution process in the Ir@$SrIrO_3$ heterojunction region. Reproduced with permission from Ref. [55], © Zhao, L. et al. 2024. (b) Preparation of the Pt/TiO_2 catalyst. Reproduced with permission from Ref. [57], © Wu, Z. et al. 2023. (c) Preparation of the Pt_1/Co single atom array (SAA) catalyst via ball milling. Reproduced with permission from Ref. [58], © American Chemical Society 2020.

In addition, microwave synthesis has high value in reducing energy consumption and avoiding agglomeration [56]. Wu et al. [57] pioneered the design of oxidation vacancies (O_V) rich black titanium dioxide loaded with sub nanometer Pt clusters (Pt/TiO_2-O_V) through solvent free microwave treatment and subsequent low temperature nonplating process, and realized metal–support interaction (Fig. 1(b)). This process does not require high temperature and strong reducing agents, which can effectively avoid the agglomeration of Pt species.

Similarly, ball milling as a simple, economical and environmentally friendly preparation method has also been used to prepare noble metal single atom catalysts (SACs). Recently, Ji and co-workers [58] successfully prepared Pt_1/Co platinum cobalt single atom alloy catalysts by ball milling, and realized kilogram scale production of Pt_1/Co (Fig. 1(c)). By applying different M_1/Co (M = Pt, Pd, Ru, Ir, and Rh) single atom alloy catalysts to the selective hydrogenation reaction of 5-hydroxymethylfurfural (HMF), the Pt_1/Co catalyst showed the highest catalytic activity. Under the conditions of 180 °C and 1.0 MPa H_2 for 2 h, HMF could achieve 100% conversion, and N,N-dimethylformamide (DMF) selectivity could reach 92.9%. These research results provide new ideas and methods for the industrial application of noble metal SACs.

It is worth noting that the large-scale application of metal nanocatalysts not only relies on the improvement of synthesis controllability but also needs to keep up with the development trend of green chemistry. Through paths, such as atomic economy optimization, selection of environmentally friendly solvents, and reduction of energy consumption, the dual goals of sustainability and cost control in the synthesis process can be achieved. In terms of atomic economy methods, such as ball milling and electrochemical atomic exfoliation, can reduce by product formation through directional conversion or precise removal strategies and the atomic utilization rate is close to the theoretical upper limit [59, 60]. In terms of the application of environmentally friendly solvents solvent free synthesis strategy has become an important breakthrough direction. However, electrochemical atomic exfoliation, top-down dissolution, and other methods still rely on organic electrolytes or special eluents. Such reagents are difficult to recycle and easily cause environmental burden, so the development of aqueous phase systems or recyclable solvent formulations has become a key point [61]. In terms of energy consumption, control microwave synthesis, low temperature oil phase strategy, and other methods greatly reduce the reaction activation energy by enhancing energy utilization efficiency. However, the energy consumption of industrial scale atomic layer deposition equipment is three times that of traditional roasting processes, and it is still necessary to optimize the equipment structure and energy recovery system [62].

The optimization of future synthesis methods needs to further strengthen the green chemistry orientation. Develop non-toxic and degradable metal precursors in atomic layer deposition technology to reduce process environmental risks. Optimize the electrolyte composition in electrochemical atomic regulation methods and adopt aqueous phase systems to replace organic electrolytes. Further improve atomic economy and energy consumption efficiency through multi method coupling, such as microwave assisted ball milling. At the same time, establish a green evaluation system for the entire process of catalyst synthesis, incorporating solvent toxicity, energy consumption, waste output, and other factors into consideration. Promote the development of catalyst synthesis towards a sustainable direction with low emission, low energy consumption, and high atomic utilization rate. This not only reduces the environmental cost in the industrialization process but also meets the requirements of the global green transformation of chemical processes. The summary is shown in Table 1.

2.2 Surface atomic migration and reconfiguration

Under high temperature or reaction atmosphere, surface atoms of metal nanoparticles are prone to migration and reconstruction, which is one of the key factors restricting catalyst stability [63]. For example, Li and co-workers [64] found that nickel (Ni) in PtNi nanoalloys and zinc (Zn) on zeolitic imidazolate framework-8 (ZIF-8) derived nitrogen doped carbon (Zn1-CN) supports underwent metal atom exchange at high temperature, generating PtZn nanocrystals and Ni single atoms (Ni1-CN). The $(PtZn)_n$/Ni1-CN multi-site catalyst showed low CO_2 protonation and CO desorption energy barriers in the carbon dioxide reduction reaction (CO_2RR), greatly improving the catalytic performance of CO_2RR. This dynamic evolution not only affects catalytic performance but may also cause catalyst deactivation. Liu and co-workers [65] found that the Ir_1Cu_1 dual atom catalyst would undergo reversible structural evolution of agglomeration and redispersion during high temperature reactions, and its activity could be restored through oxidative regeneration, but the long-term stability of this mechanism still needs further research. This discovery reveals the dynamic behavior of metal nanocatalysts under reaction conditions, providing new ideas for designing catalysts with self-healing ability.

Surface reconstruction is a common phenomenon of catalysts under reaction conditions. Metal nanoparticles may undergo changes in shape, surface structure, composition, and atomic arrangement in response to the pressure, temperature of reactant or product gases, and the reaction between the catalyst surface and gases. Metal oxide supports may also partially or completely encapsulate metal nanoparticles, changing their electronic structure and reactivity. Therefore, the rational design of catalysts must consider that these reconstructions may occur under reaction or catalytic conditions, and understand how they happen.

Recent studies have also found that the migration and reconstruction of surface atoms can be regulated through surface ligand engineering. The surface of metal nanomaterials is usually protected by surface stabilizing ligands, which can affect the structure and performance of catalysts. Surface organic ligands may reduce the activity of electrocatalysts, while ligand detachment will lead to the collapse of the original structure and decrease in selectivity. Therefore, it is necessary to balance the stability and activity of ligands [66–68].

3 Challenges in structural stability under dynamic conditions

Although atomic scale precise regulation technology has made phased progress in the optimization of synthesis methods and the regulation of surface atomic migration, the practical application scenarios of catalysts are often accompanied by dynamic conditions, such as high temperature, strong oxidizing or acidic atmosphere, and continuous action of reactant or product molecules. The above technical bottlenecks mainly focus on the difficulties of atomic arrangement and structure control in the static preparation process. In real catalytic reaction systems, the surface atoms of catalysts will further face more complex stability

Table 1 Comparison of core limitations and solution approaches for different synthesis methods

Synthesis method	Limitations	Solutions
ALD	Controllability: Large mass transfer resistance in the pores of complex supports leads to uneven distribution of metal atoms. Scalability: controllable at small laboratory scale, but uniformity decreases after scaling up. Cost: high price of special precursors and large initial investment in equipment. Industrial feasibility: difficult to achieve precise regulation in pores, making it hard to mass-produce uniform products	Optimize the reactivity of precursors and design the mass transfer structure of pores for industrial-scale ALD equipment; combine machine learning to predict deposition paths
Liquid/plasma etching	Controllability: cannot achieve precise single atom removal, easily causing disordered surface defects. Scalability: fluctuations in etching rate during large-scale production result in poor product consistency. Cost: high energy consumption of plasma equipment and difficulty in recycling liquid etchants. Industrial feasibility: insufficient precision to meet the requirements of atomic level structure regulation	Introduce electrochemically assisted etching technology to regulate the concentration gradient of etchants; develop recyclable and environmentally friendly etching systems
Electrochemical atomic exfoliation	Controllability: relies on precise control of potential and time, and impurities are likely to interfere with selectivity. Scalability: only applicable to a few alloy systems, with poor adaptability to multi-metal catalytic systems. Cost: high investment in special electrochemical equipment and high cost of high-purity raw materials. Industrial feasibility: immature electrolyte recovery system and insufficient long-term operation stability	Develop universal electrolyte formulations to expand the adaptability to alloys and single metals; optimize the automatic control module of equipment to reduce energy consumption
Top-down dissolution method	Controllability: strict requirements on the crystal structure of supports, only applicable to specific perovskite supports. Scalability: narrow process window for dissolution conditions (temperature, concentration), which is easy to lose control during scaling up. Cost: high price of precursors for specific supports. Industrial feasibility: poor adaptability to supports, unable to be extended to carbon-based and general oxide supports	Develop multi-functional composite leaching agents to reduce the dependence on support structures; combine *in situ* characterization to real-time regulate the dissolution process
Microwave synthesis	Controllability: local hotspots lead to agglomeration of metal species when scaling up to gram level or above. Scalability: uneven distribution of microwave field results in decreased product dispersibility during mass production. Cost: high energy consumption of industrial-scale microwave equipment and limited adaptability of solvent-free processes. Industrial feasibility: difficult to control product uniformity and insufficient long-term operation stability	Design multi-cavity uniform microwave field equipment; couple ultrasonic-assisted dispersion to suppress local hotspots; expand solvent-free large-scale processes
Ball milling method	Controllability: high requirements on the lattice matching degree of metal components, and single atoms are prone to uneven distribution. Scalability: wear of grinding media introduces impurities during large-scale production. Cost: low equipment cost, but high loss rate of high-purity metal raw materials. Industrial feasibility: impurity content of products (grinding media debris) affects catalytic performance	Adopt wear-resistant ceramic or polymer grinding media; predict metal lattice matching degree through DFT to precisely design alloy components; develop online impurity filtration processes

challenges, such as dissolution, sintering, and imbalance of support interaction. The structural evolution caused by these dynamic environments directly offsets the performance advantages brought by precise synthesis and becomes the key obstacle restricting the practical application of metal nanocatalysts. Therefore, this chapter will focus on discussing the structural stability problems of catalysts under dynamic reaction conditions, conduct in-depth analysis of core issues, such as surface atomic dissolution and sintering, and dynamic balance of support metal interaction, and summarize relevant regulation strategies, so as to provide theoretical and experimental references for breaking through the bottleneck of long-term service stability of catalysts.

3.1 Surface atomic dissolution and sintering

In strong oxidation or acidic environments, surface atoms of metal nanoparticles are prone to dissolution, which is an important factor restricting the long-term stability of catalysts. Stamenkovic and co-workers [69] revealed the dissolution trend of well-defined single crystal films and nanoscale platinum exposed surfaces through atomic scale analysis. The study found that using an Au underlayer can promote the ordered arrangement of Pt surface atoms into the (111) structure, while the surface Au layer can selectively protect low coordinated Pt sites (Figs. 2(a)–2(c)). After applying this mitigation strategy to 3 nm Pt_3Au/C nanoparticles, the Pt dissolution phenomenon in liquid electrolyte was successfully eliminated, enabling the material to achieve a 30-fold durability improvement within the extended potential range of up to 1.2 V, which is significantly better than the 3 nm Pt/C base material.

Similarly, liquid catalysts have unique anti deactivation ability. Yu et al. [24] designed a new carbon coated liquid alloy catalyst $Ga_{79}Cu_{11}Mo_{10}@C$ by activating gallium (Ga) active sites, achieving efficient electrochemical urea synthesis (Fig. 2(d)). During the synergistic reduction of nitrogen (N_2) and CO_2, the urea yield reached 28.25 $mmol{\cdot}h^{-1}{\cdot}g^{-1}$, setting the highest record under similar conditions. The Faradaic efficiency (FE) was as high as 60.6% under −0.4 V vs. reversible hydrogen electrode (RHE). In addition, the catalyst showed excellent stability in the 100 h test. Comprehensive analysis shows that the sequential exposure of high-density active sites promotes the adsorption and activation of N_2 and CO_2, realizing efficient coupling reaction. This coupling reaction forms C–N bonds through the thermodynamically spontaneous reaction between *N=N* and CO. The deformability of the liquid state promotes catalyst recovery and enhances its stability and antipoisoning ability.

In OER, the rapid oxidative dissolution of FeCoNiCu alloy is a serious problem. Wu and co-workers [70] first reported that FeCoNiCu multi element alloy nanoparticles (MEA NPs) can be stabilized with only 0.3 at.% Pd. Although pure Pd has extremely poor OER activity and durability, Pd-FeCoNiCu can be maintained for 1000 h at 10 $mA{\cdot}cm^{-2}$. In the accelerating durability test (ADT) at 100 $mA{\cdot}cm^{-2}$, it showed an increase of only 8.9 mV within 25 h, with a degradation rate of 0.356 $mV{\cdot}h^{-1}$, which is 1/350 of FeCoNiCu (125 $mV{\cdot}h^{-1}$) and one of the most stable OER catalysts reported so far (Figs. 2(e) and 2(f)). However, the synergistic interaction mechanism between Pd and FeCoNiCu has not been fully clarified, and the uniformity of Pd distribution is difficult to

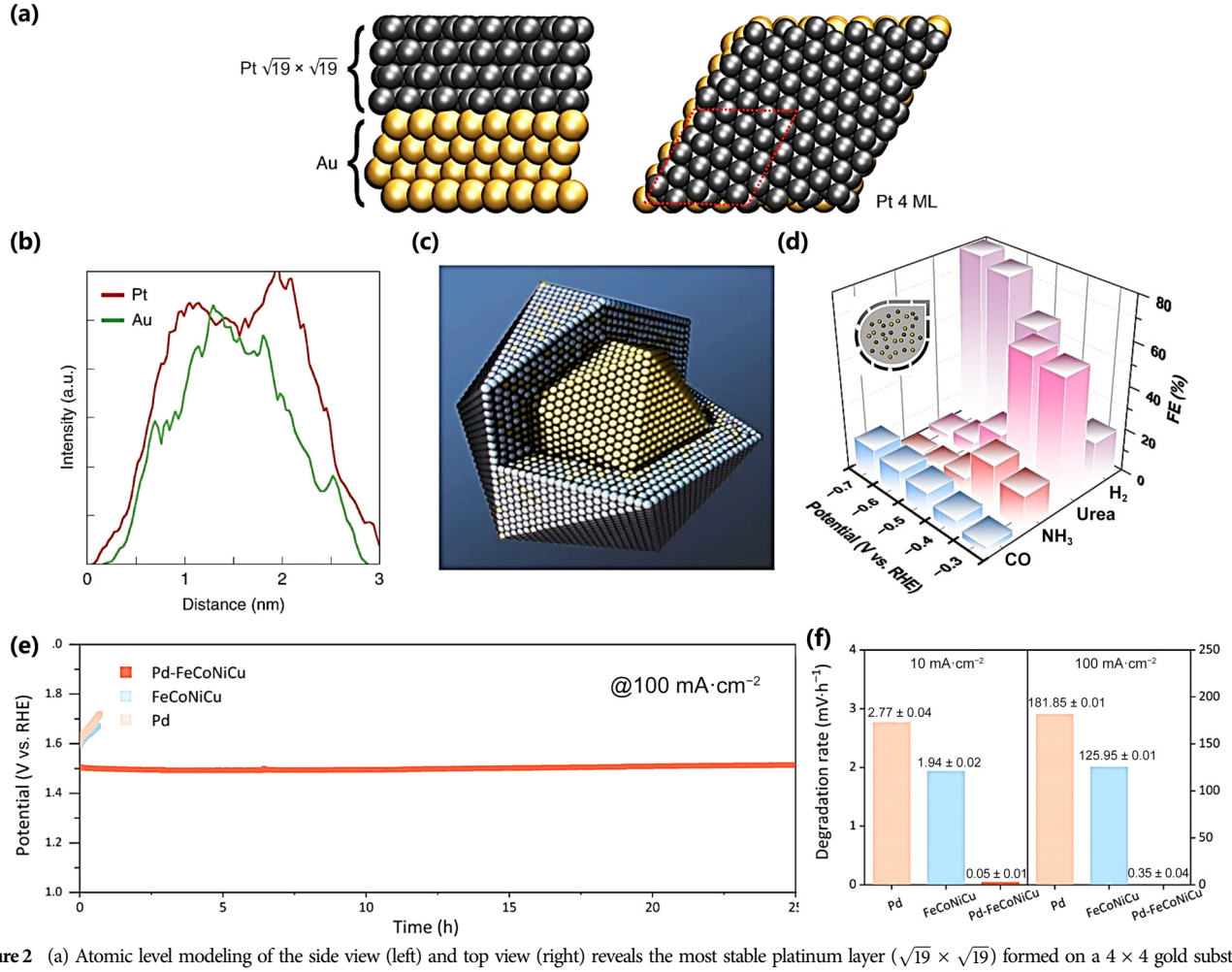

Figure 2 (a) Atomic level modeling of the side view (left) and top view (right) reveals the most stable platinum layer ($\sqrt{19} \times \sqrt{19}$) formed on a 4 × 4 gold substrate. (b) Energy-dispersive X-ray spectroscopy line scans demonstrate a gold-enriched core encapsulating a platinum shell layer. (c) Schematic of the platinum-gold core–shell nanoparticle exhibiting a distinct compositional gradient distribution. Reproduced with permission from Ref. [69], © Lopes, P. P. et al. 2020. (d) Faradaic efficiency distribution of $Ga_{79}Cu_{11}Mo_{10}$@C at different potentials using nitrogen and carbon dioxide as feed gases. Reproduced with permission from Ref. [24], © Wiley-VCH GmbH 2024. ((e) and (f)) Stability testing of Pd-FeCoNiCu, FeCoNiCu, and Pd at (e) 100 mA·cm^{-2} under 1 M KOH solution and (f) Degradation rates during ADT at 10 and 100 mA·cm^{-2}. Reproduced with permission from Ref. [70], © American Chemical Society 2025.

control precisely; in strong oxidizing environments, the dissolution of elements, such as Fe, Co, and Ni, still cannot be completely inhibited but only delayed, and the composition and structure of the catalyst will undergo irreversible changes after long term use; the preparation process of multi element alloys is complex, which requires precise control of the proportion of each metal component and reaction conditions, making it difficult to realize large scale production.

In addition, Ostwald ripening of metal atoms at high temperature will lead to an increase in particle size and a sharp decrease in active surface area. Zeng and co-workers [71] developed a cerium oxide nano island (CeO_x) modified copper oxide catalyst (CuO) by constructing a nano island structure, which is characterized by CeO_x uniformly distributed on the surface of CuO nanoparticles in the form of isolated nano islands (Fig. 3). When the CuO substrate is reduced to metallic Cu, the CeO_x layer can effectively stabilize the CuO_x at the interface and prevent its further reduction. Using metal oxide clusters to isolate metal particles can effectively inhibit sintering, but this method has strict requirements on the selection of supports and preparation processes. However, this method is highly dependent on the deposition parameters during the preparation process (such as temperature, concentration, and time), and the process window is narrow. The interfacial interaction between CeO_x and CuO is weak. During high temperature reactions, the migration and agglomeration of CeO_x nano islands are prone to occur, leading to the loss of the stabilizing effect on Cu species.

Fe-N-C catalysts are the most promising non noble metal ORR catalysts to replace Pt, but the practical application of current high activity Fe-N-C catalysts is still limited by their insufficient stability. Studies have shown that the deactivation mechanisms of Fe-N-C catalysts mainly include demetallization, carbon oxidation, protonation, and microporous water flooding.

To solve these problems, researchers have proposed various life extension strategies, including constructing stable carbon supports, constructing stable active sites, and avoiding Fenton reactions. For example, by using carbon materials with high graphitization degree as supports, the oxidation resistance of carbon supports can be improved [72]; by introducing nitrogen doping or other heteroatoms, the stability of active sites can be enhanced [73]; by controlling the loading and distribution of iron (Fe) or other metals, the occurrence of Fenton reactions can be reduced [74–76].

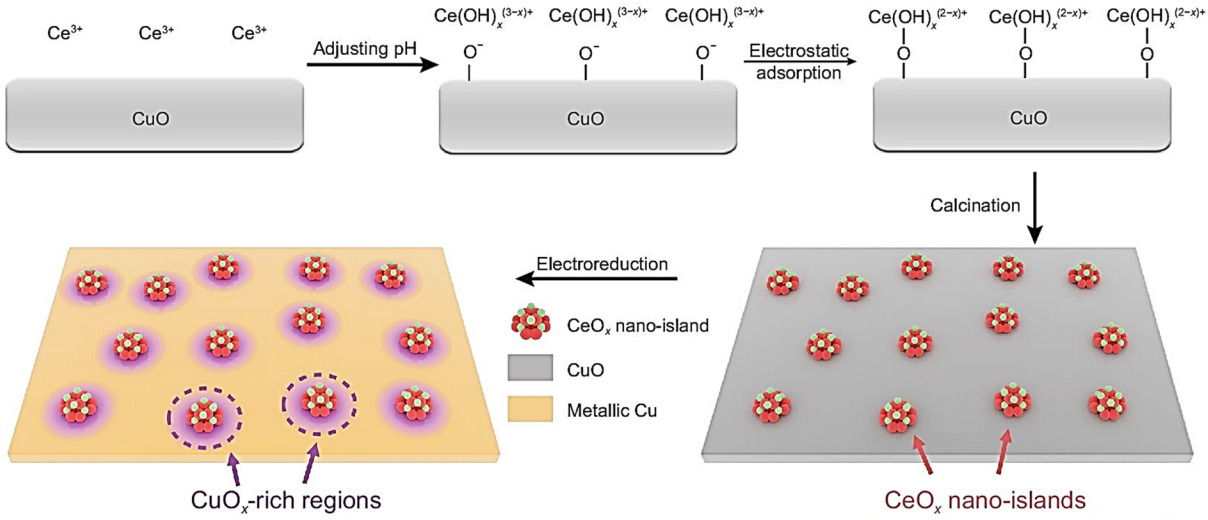

Figure 3 Schematic of electrostatic adsorption synthesis and CeO_x nanoislands after *in situ* electrochemical reduction, along with the introduced CuO_x-rich regions. Reproduced with permission from Ref. [71], © Wei, M. et al. 2025.

3.2 Dynamic equilibrium of metal–support interactions

The strong metal support interaction (SMSI) can stabilize metal atoms, but changes in reaction conditions may break this balance. Fortunelli and co-workers [77] successfully designed a CoO_x@Pt/C nanocatalyst with both activity and stability. By embedding dispersed CoO_x clusters into tiny Pt nanoparticles, each CoO_x cluster is completely protected by a Pt shell. This oxide embedded design makes full use of the strong interaction between Pt and oxide, enabling the catalyst to have high structural and chemical stability without sacrificing activity. The initial mass activity of CoO_x@Pt nanocatalyst is 1.10 $A{\cdot}mg_{Pt}^{-1}$, the rated power density is 1.04 $W{\cdot}cm^{-2}$, and the Pt utilization rate in the membrane electrode assembly is 10.4 $W{\cdot}mg_{Pt}^{-1}$. Yet, the thickness and uniformity of Pt shell layers are difficult to control precisely. After the catalyst is discarded, the separation and recovery of Pt and Co require complex chemical treatment steps, which consume high energy, have low recovery efficiency, and cause serious resource waste.

Metal oxide supports can partially or completely encapsulate metal nanoparticles, changing their electronic structure and reactivity [78]. This encapsulation phenomenon is particularly obvious under high temperature or reaction atmosphere, which may lead to partial or complete coverage of catalyst active sites, thus affecting catalytic performance. Therefore, how to avoid excessive encapsulation while maintaining the strong interaction between metal and support is the key to improving catalyst stability.

Researchers also found that the interaction between metal and support can be adjusted through surface engineering. Sun and co-workers [79] proposed a near surface regulation method. Using atomic resolution transmission electron microscopy (TEM), it was confirmed that this method can reduce the thickness of the Pt rich layer near the surface from 5–7 atomic layers to 2–3 atomic layers. It was also found that the modified catalyst not only showed significantly enhanced ORR activity (7.7 $mA{\cdot}cm_{Pt}^{-2}$ and 1.9 $A{\cdot}mg_{Pt}^{-1}$@0.9 V vs. RHE, Figs. 4(a)–4(c)), but also had good electrochemical stability. Density functional theory (DFT) revealed the essential reasons for high activity and stability: Reducing the thickness of Pt rich can reduce the adsorption energy of OH* on surface Pt. At the same time, it was found that the internal Pt rich composition will stabilize the internal Ni atoms and limit their diffusion and dissolution. After near surface structure modification, the catalyst has a unique near surface structure and internal composition, breaking the development bottleneck that octahedral Pt Ni catalysts have difficulty achieving both activity and stability. While, its applicability to Pt based alloys with other morphologies (such as cubes and spheres) or compositions (such as Pt–Co and Pt–Fe) is unknown, and precise particle by particle regulation cannot be achieved in industrial production.

In addition, surface ligand engineering is also used to adjust the interaction between metal and support. By selecting appropriate ligands, the dispersion and stability of metal nanoparticles on the support surface can be controlled, thereby improving the overall performance of the catalyst. For example, Hong and co-workers [80] innovatively modified Ni_2Cl_2BTDD (BTDD = bis(1H-1,2,3-triazolo[4,5-b], [4',5'-i]) dibenzo [1,4]dioxin), hereafter referred to as Ni_Cl, via post-synthesis triazole ligand exchange (specifically 1,2,4-triazolate (tz) and 3,5-dimethyl-1,2,4-triazolate (dmtz)). This approach retained open metal sites while introducing synergistic CO_2 adsorption sites, enabling the modified Ni_dmtz to exhibit 2.5 times increase in CO_2 adsorption capacity, high CO_2/N_2 selectivity, and significantly enhanced stability in humid environments (Figs. 4(d)–4(f)).

3.3 Dual functions and regulation of dynamic encapsulation strategy

Dynamic encapsulation refers to constructing a coating layer with response ability to reaction conditions on the surface of metal nanocatalysts, such as oxide clusters, carbon layers, coordination polymers, and alloy surface layers. This coating layer is not a static inert barrier but a core strategy that can adaptively adjust its structural morphology and interface interaction strength with the reaction environment, such as temperature, atmosphere, and potential, and affect the catalyst stability and reaction performance through the synergistic effect of dynamic protection and activity regulation. Different from traditional static encapsulation, such as oxide coatings with fixed thickness, the core feature of dynamic encapsulation lies in that the coating layer can adapt to the needs of each reaction stage through dynamic processes, such as dissolution, redeposition, redox reactions, and conformational changes. This is also the key characteristic that distinguishes it from surface defect engineering and interface regulation.

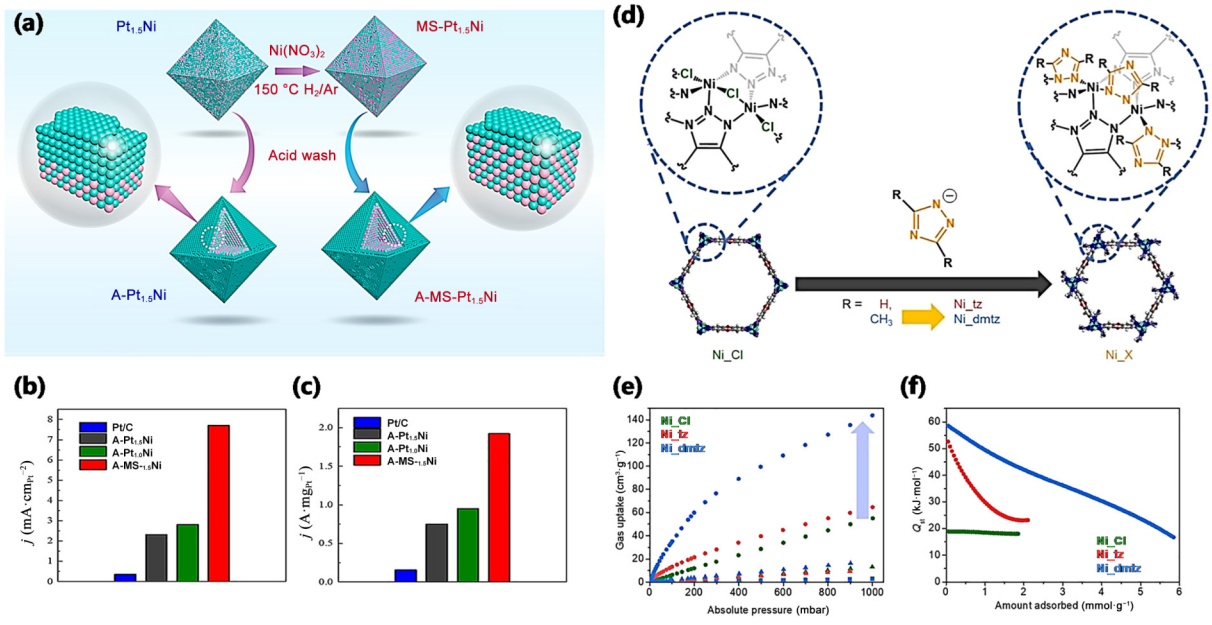

Figure 4 (a) Schematic of the synthesis routes for A-$Pt_{1.5}$Ni, MS-$Pt_{1.5}$Ni, and A-MS-$Pt_{1.5}$Ni, Pt (green), Ni (pink). (b) Specific activity and (c) mass activity of Pt/C, A-$Pt_{1.5}$Ni, A-$Pt_{1.0}$Ni, and A-MS-$Pt_{1.5}$Ni at a potential of 0.9 V vs. RHE. Reproduced with permission from Ref. [79], © American Chemical Society 2020. (d) Structures of Ni_Cl and bridge-ligand-modified Ni_tz and Ni_dmtz. Ni (green), N (blue), C (gray), H (white), and Cl (purple). (e) Adsorption isotherms of CO_2 (circles), N_2 (squares), and CH_4 (triangles) at 298 K for Ni_tz (red), Ni_dmtz (blue), and Ni_Cl (green). (f) Adsorption isotherms (the isosteric heats of adsorption (Q_{st})) for Ni_Cl, Ni_tz, and Ni_dmtz. Reproduced with permission from Ref. [80], © American Chemical Society 2025.

As an important means for structural stability regulation, the double-edged sword effect of dynamic encapsulation is reflected in two aspects:

(1) Precise stabilization of catalytic structure. On the one hand, the dynamic encapsulation layer can physically isolate the catalyst surface from the reaction medium and inhibit atomic sintering at high temperatures and metal atom dissolution in strong acid or alkali environments [81, 82]. On the other hand, the dynamic electronic coupling between the coating layer and the metal surface can regulate the electronic structure of active sites and achieve the synergistic improvement of activity and stability [83–85]. In addition, some dynamic encapsulation layers, such as flexible coordination polymers, can capture migrating surface atoms through conformational changes inhibit reconstruction induced deactivation, and even realize self-repair of active sites [86, 87].

(2) Active site shielding and mass transfer limitation. Improper regulation of the thickness or structure of the dynamic encapsulation layer will cause significant negative effects. First, excessive encapsulation leads to physical shielding of active sites and blocks the contact between reactants and active centers [88]. Second, the dynamic reconstruction of the coating layer may change the pore structure and increase mass transfer resistance [89, 90]. Third, some coating layers, such as metal oxides, may undergo excessive reduction or oxidation during the reaction, leading to imbalance of interface interaction and instead accelerating catalyst deactivation [91–93].

The core regulatory goal of the dynamic encapsulation strategy is to balance the protective effect and activity release through precise design of the composition thickness and response mechanism of the coating layer. For noble metal catalysts that are prone to dissolution and sintering, thin high activity coating layers can be used to inhibit atomic loss while maintaining the exposure degree of active sites [94]. For liquid or easily reconstructed catalysts, such as liquid alloys, flexible adaptive coating layers can be selected to optimize mass transfer through pore structure and adapt to the dynamic structure of the catalyst through the deformability of the coating layer [95, 96].

4 Precision challenges in active site design

4.1 Limitations of single atom anchoring

The activity of SACs is highly dependent on the anchoring sites on the support surface. Traditional views hold that surface defects are the main anchoring positions, but He and co-workers [97] found that terminal hydroxyl groups rather than defects on the surface of reducible support CeO_2 are the direct anchoring sites for single atom Ag. They further proposed a universal anchoring mechanism for noble metal atoms (Pt, Pd, and Ag) on CeO_2. This finding revises traditional understanding, but the stability of hydroxyl groups is affected by pH and temperature, which limits the application range of SACs (Figs. 5(a)–5(f)).

In addition, the random distribution of SACs leads to uneven coordination environments, affecting catalytic selectivity. To solve this problem, researchers have developed various strategies to control the distribution and coordination environment of single atoms. For example, Wu and co-workers [98] developed a strategy of shrinkage induced by self-assembly and synthesized one-dimensional (1D) single atom arrays (Fig. 5(g)). By controlling experimental conditions, they analyzed the specific formation process and influencing factors of the array. Using advanced electron microscopy techniques, they observed that the array consists of stripes periodically arranged parallel to the nanosheet surface. Each stripe comprises numerous graphene sheets vertically distributed on the nanosheet surface, with most metal atoms anchored within the graphene. Ultimately, the metal atoms exhibit one-dimensional ordered distribution at the microscale. In addition, the contraction induced self-assembly strategy is

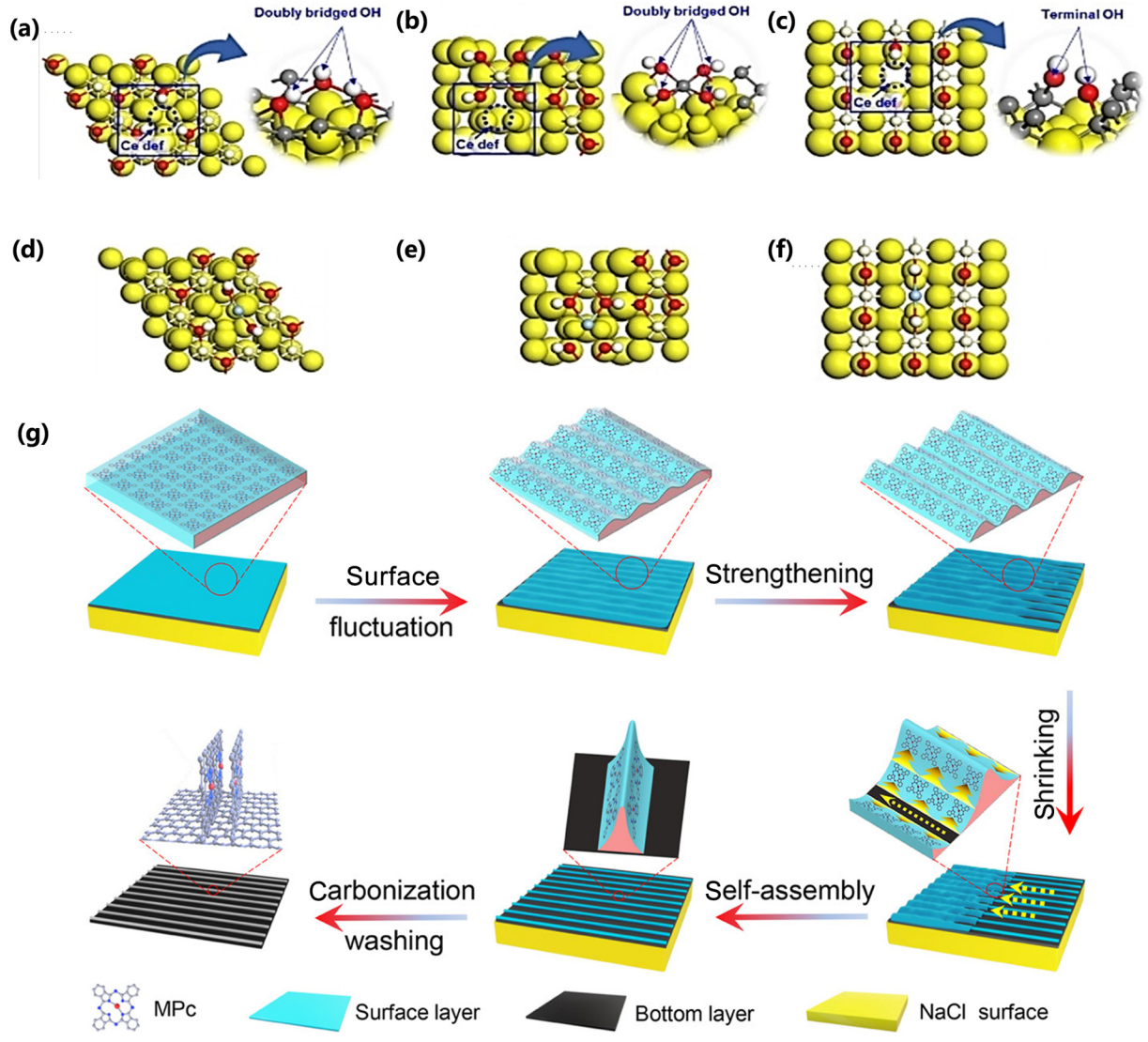

Figure 5 ((a)–(c)) Optimized geometric configurations of hydroxylated defects on (111), (110), and (100) surfaces; red and white spheres represent oxygen and hydrogen atoms; gray spheres (right panel) denote the CeO_2 top layer surrounding vacancy defects; large spheres represent the CeO_2 sheet substrate (yellow); and Ce vacancy defects (dashed circles). ((d)–(f)) Optimized geometric configurations of Ag adsorbed on CeO_2 (111), (110), and (100) surfaces, with corresponding binding energies and binding configurations. O (red), H (white), Ag (blue), CeO_2 sheet substrate (yellow). Reproduced with permission from Ref. [97], © Wang, F. et al. 2024. (g) Schematic of one-dimensional SAA synthesis. Reproduced with permission from Ref. [98], © American Chemical Society 2022.

extremely sensitive to experimental conditions (such as temperature, concentration, and solvent), and it is difficult to realize uniform replication of array structures on a large scale.

4.2 Difficulty in regulating multi-site synergistic effects

The synergistic effect of active sites (such as diatomic sites or heterogeneous trimers) can significantly improve catalytic performance, but precisely designing the geometric and electronic structures of these sites is extremely challenging. For example, the Pt–Fe–Pt heterogeneous trimer constructed by Shen and co-workers [99] has densely distributed and precisely arranged Pt atoms. It not only catalyzes the preferential hydrogenation of the C=O bond in crotonaldehyde (CAL) but also increases the reaction rate by 35 times, avoiding the trade-off between catalytic activity and product selectivity. However, the universality and long-term stability of this structure still need optimization. Ye and co-workers [100] developed and synthesized a series of magnesium-rich intermetallic compounds $Mg_{29}TM_4$ (TM = Pd, rhodium (Rh), and iridium (Ir), Pt). By periodically isolating TM atoms to form ordered single atom structures, they achieved high activity and selectivity in acetylene semi-hydrogenation and olefin hydroformylation reactions (Figs. 6(a) and 6(b)). Meanwhile, the ternary catalyst $Mg_{29}Pd_{1.3}Rh_{2.7}$ uses the electron transfer effect of magnesium (Mg) to construct electron-rich active centers, cooperating with Pd and Rh single atom sites. It successfully realizes the phenylacetylene hydrogenation–hydroformylation cascade reaction, showing great potential for atomic level tandem catalysis. But this method has strict restrictions on the types of metals and the selection of supports.

Besides the precise arrangement of geometric structures, the spin configuration in electronic structures is an easily overlooked yet key regulatory dimension. It directly affects catalytic activity and selectivity through mechanisms, such as optimizing the adsorption energy of reaction intermediates and reducing the spin flip energy barrier.

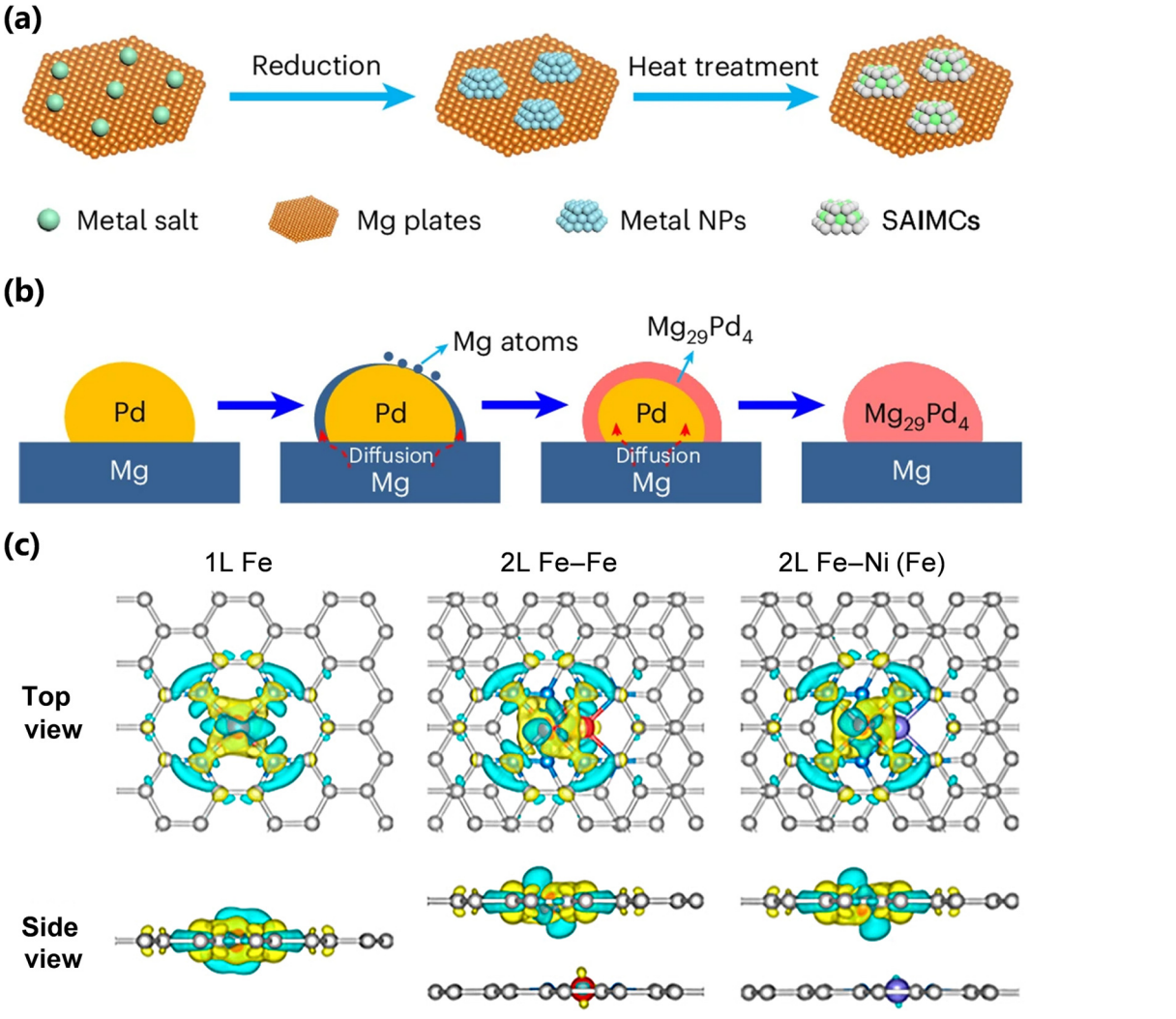

Figure 6 (a) Preparation process of $Mg_{29}TM_4$. (b) Evolution of $Mg_{29}TM_4$ formation. Reproduced with permission from Ref. [100], © Lu, X. et al. 2025. (c) Charge density differences for 1L Fe, 2L Fe–Fe, and 2L Fe–Ni (Fe). Yellow and cyan represent electron-enriched and depleted regions. Reproduced with permission from Ref. [109], © American Chemical Society 2023.

In the oxygen reduction reaction, the regulatory effect of spin configuration on the reaction path is particularly significant. Huang and co-workers [101] reported a phosphorus-bridged Fe single atom/atomic cluster (AC) composite catalyst ($Fe_{SA/AC}$/PNC). The unique Fe_{SA}-P-Fe_{AC} structure not only acts as an electron channel but also successfully induces the spin state of Fe^{II} to transform from low spin (S = 0, S denotes the spin state) to intermediate spin (S = 1). This spin reconstruction optimizes the adsorption strength of key oxygen intermediates by regulating orbital occupation, significantly improving the ORR performance in acidic and neutral media. Liu and co-workers [102] precisely anchored platinum Pt nanocrystals on atomically dispersed Fe-N-C substrates (Pt/Fe-N-C) through an interface engineering strategy, controlling the Pt particle size (2–8 nm) precisely.

In nitrogen reduction reaction and water splitting reaction, spin state transition also plays a key role. Wang and co-workers [103] proposed and verified a new viewpoint that low spin Fe sites promote N_2 activation. Through a synergistic strategy of amorphous TiO_2 phase transition and F doping, continuous regulation of the spin state of single atom Fe is achieved, greatly reducing the Fe magnetic moment. Combined with DFT calculations and *in situ* diffuse reflectance infrared Fourier transform spectroscopy (DRIFTS), it is revealed that the formation of N–NH* intermediate and NH_3 desorption are key steps, and low spin Fe significantly reduces their free energy barriers. Yan and co-workers [104] prepared a core–shell structured catalyst composed of antiferromagnetic $YFe_{1-x}Mn_xO_3$ core and paramagnetic YFeOOH shell ($YFe_{1-x}Mn_xO_3$@YFeOOH). This catalyst effectively eliminates the electron scattering effect caused by opposite magnetic moments in the system, reduces the spin flip energy barrier for electron transfer, breaks through the limitation of linear Arrhenius kinetics that the catalytic reaction rate follows the thermal diffusion effect with system temperature, and achieves the electrothermal energy coupled catalytic enhancement effect.

Diversified strategies for spin configuration regulation have been formed, including element doping [105, 106], coordination environment modification [107], and external field regulation [108]. These studies collectively confirm that, as a core dimension of electronic states, the precise regulation of spin configuration is the key to breaking through the kinetic bottleneck of multi-site synergistic catalysis, providing a brand new paradigm for the rational design of active sites.

Recently, researchers also diffused different metal phthalocyanine molecules (NiPc and FePc) along the NaCl surface into thin films. Following further carbonization, the aggregates transformed into vertically aligned multilayer graphene, forming parallel stripes [109]. The abundant N defects in graphene can co-center Ni and Fe atoms in three-dimensional space (Fig. 6(c)), facilitating the generation of high-density axial Ni- and Fe-based double-atom sites (NiFe DAS). These findings provide both theoretical foundations and experimental evidence for designing highly efficient dual- or multi-center catalysts.

In addition, high-entropy alloys (HEAs) have attracted wide attention in the field of electrocatalysis due to their unique advantages (tunable composition, complex surface, high tolerance, etc.) [13, 14]. They can form new and customizable active sites between adjacent multi-elements, and their interactions can be regulated by rational selection of element configuration and composition [25, 27, 35]. Li et al. [110] synthesized uniform and ultra-small (~ 3.4 nm) high entropy alloy $Pt_{18}Ni_{26}Fe_{15}Co_{14}Cu_{27}$ nanoparticles through a simple atmospheric pressure low-temperature oil-phase strategy. The $Pt_{18}Ni_{26}Fe_{15}Co_{14}Cu_{27}$/C catalyst exhibits an ultra-small overpotential of 11 mV at a current density of 10 $mA{\cdot}cm^{-2}$, as well as excellent activity (10.96 $A{\cdot}mg_{Pt}^{-1}$ at a potential of −0.07 V vs. RHE) and stability in alkaline media. Periodic density functional theory calculations confirm that multiple active sites for both the HER and methanol oxidation reaction (MOR) exist on the HEA surface, which are key factors for proton and intermediate conversion. At the same time, the structure of the HEA surface provides rapid inter-site electron transfer for reduction and oxidation processes.

5 Insufficient dynamic monitoring of characterization technologies

5.1 Spatiotemporal resolution limitations of in-situ characterization

Although existing *in situ* TEM and synchrotron radiation technologies can observe the structural evolution of catalysts during reactions, their time resolution (second level) makes it difficult to capture atomic level transient changes. Zhong and co-workers [111] explored the dynamic lattice strain of nanoalloy catalysts formed by alloying dual noble metals with earth-abundant metals (such as Ni or Co) under working conditions. They found that during the surface dealloying process, there is oscillatory lattice strain in the alloy nanoparticles triggered by interfacial reactions. By analyzing the lattice strain through time frequency domain transformation and theoretical calculations, the origin of this strain was revealed to be the diffusion path of metal atom vacancies to promote realloying after dealloying.

In addition, the electronic state of surface atoms (such as spin configuration) is crucial for catalytic performance, but conventional X-ray absorption spectroscopy (XAS) is difficult to achieve dynamic tracking. This limitation makes it difficult for researchers to observe the dynamic changes of surface atoms of catalysts in real time during reactions, thereby affecting the understanding of catalytic mechanisms and the rational design of catalysts.

To solve these problems, researchers are developing *in situ* characterization technologies, such as the combination of *in situ* electron microscopy and *in situ* Raman/infrared spectroscopy, to realize real-time dynamic tracking of catalyst structure, electronic state, and reaction intermediates [97]. Researchers have also used the fractal box counting dimension to characterize the surface roughness of metal nanoparticles [112, 113]. This method is different from the traditional concept of roughness but provides a new indicator for the functional properties (such as catalytic performance) of catalysts, which was previously unavailable. Studies have found that although it is difficult to consistently correlate the fractal dimension with the catalytic activity of surface crystal planes, a matching trend with surface energy, thermodynamic stability, and the number of bond vacancies can be observed. This research result indicates that the fractal box counting dimension may be used to rationalize the catalytic activity trends among metal nanoparticles and provides an opportunity for designing better performing nanocatalysts through surface engineering.

5.2 Precise localization and quantification of active sites

Aberration corrected scanning TEM (AC-STEM) can observe the distribution of single atoms, but it is hard to tell surface atoms apart from bulk atoms. X-ray photoelectron spectroscopy (XPS) can analyze the chemical state of surface elements, but its signal depth is limited and cannot reflect the internal structure of catalysts. To solve these problems, researchers are developing more advanced characterization technologies and methods. Synchrotron radiation X-ray absorption fine structure spectroscopy (XAFS) can accurately determine the local structure and coordination environment of metal atoms [114–116]. Scanning tunneling microscopy (STM) can directly observe the arrangement and defects of surface atoms; [117] *In situ* infrared spectroscopy and Raman spectroscopy can monitor the formation and transformation of reaction intermediates in real-time [118, 119].

In addition, researchers have developed various calculation methods to assist experimental characterization. DFT calculations can predict the structure and electronic properties of catalyst surfaces, helping to understand catalytic mechanisms. Machine learning methods can find patterns from a large amount of experimental data, predict catalyst performance, and guide catalyst design.

6 Cost and scalability barriers to industrial application

6.1 Noble metal utilization and cost pressure

The high cost of noble metals limits their large-scale application. Although SACs can increase atomic utilization to nearly 100%, the selection of supports (such as nitrogen doped carbon or oxides) and preparation processes (such as ultrafast synthesis) still need optimization to reduce costs.

The pulse discharge method developed by Chen and co-workers [120] is used to precisely construct ruthenium copper dual atom catalysts supported on nitrogen doped graphene aerogels (RuCu DAs/NGA), providing possibilities for efficient preparation (Fig. 7(a)). However, the energy consumption and equipment investment of this method still need evaluation. In addition, Baek and co-workers [121] can prepare SACs (including Fe, Co, Ni, and Cu) through a top down abrasion method. This method directly atomizes and deposits bulk metals onto supports, such as carbon frameworks, oxides, and nitrides (Fig. 7(b)). The metal loading can be easily adjusted by changing the grinding rate. This process does not require any synthetic chemicals, solvents or even water, and

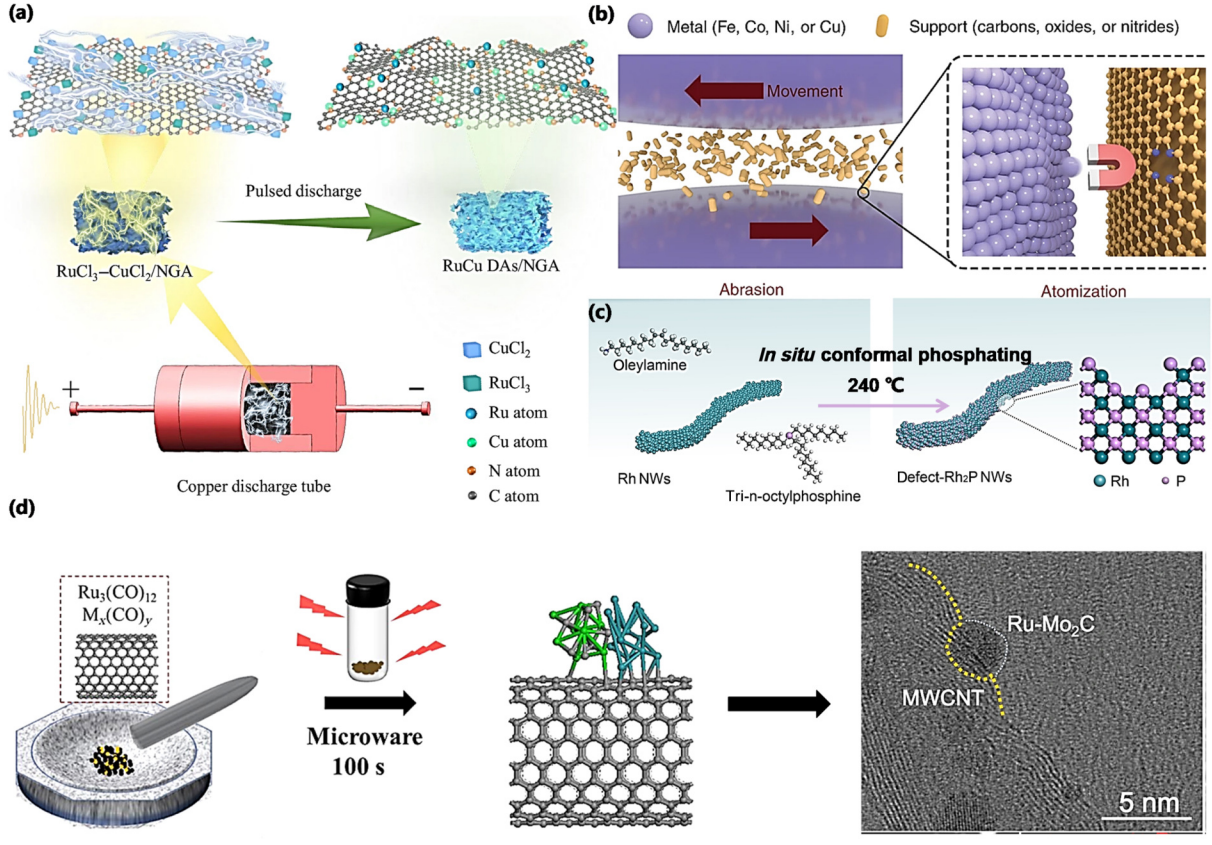

Figure 7 (a) Schematic of the pulse discharge preparation strategy. Reproduced with permission from Ref. [120], © Liu, K. et al. 2025. (b) Transformed iron atoms migrate out of defects via a transition mechanism. Nitrogen atoms subsequently capture the iron atoms, playing a crucial role in this process. Reproduced with permission from Ref. [121], © Han, G.-F. et al. 2022. (c) Schematic of the synthesis process for obtaining d-Rh_2P nanowires. Reproduced with permission from Ref. [128], © Wiley-VCH GmbH 2023. (d) Schematic of the synthesis process for Ru-Mo_xC@CNT and its high-resolution TEM (HRTEM) image, Mo (green), Ru (blue), and C (gray). Reproduced with permission from Ref. [124], © Wu, X. et al. 2021.

produces no by products or waste. Its reaction mechanism is that mechanochemical forces form defects on the support *in situ*, which then capture and stably seal the atomized metals.

Researchers have also developed a series of high-performance alloy catalysts by alloying noble metals with non-noble metals. For example, Gao and co-workers [122] developed an interface reduction method involving active hydrogen (H*) to synthesize alloy nanostructures. By adding HNO_2 into the reaction system, H* can be generated at the metal seed/solution interface, forming a strong reducing environment. The metal reduction reaction thus shifts from the solution phase to the interface. As a strong reducing agent, H* can offset the impact of differences in metal salt reduction potentials, achieving effective synergistic reduction.

6.2 Complexity of process scaling

Highly active catalysts synthesized in laboratories are easily affected by mass transfer, heat transfer, and impurities during scaling. Similarly, the regeneration and recovery technologies of catalysts are not yet mature, further increasing industrialization costs.

To solve these problems, researchers are developing more efficient and economical synthesis methods and processes. For example, Xiong and co-workers [123] designed a titanium dioxide photocatalyst loaded with Pd clusters (1Pd/TiO_2) together with a mass transfer enhanced gas–liquid–solid Taylor flow reactor. This system maintains a yield decay of less than 10% after 50 h of continuous operation, with a formamide yield as high as 256.80 μmol·h^{-1} (6.83 times higher than batch reactors). This performance is significantly better than the current most advanced photocatalytic systems for synthesizing C–N compounds from C1 small molecules. Compared with batch reactors, the core advantages of continuous flow reactors are reflected in three aspects: (1) avoid problems, such as local concentration inhomogeneity and large temperature gradients, and greatly improve the uniformity of product size and structural stability; (2) the continuous operation characteristic enables 24 h non-stop production, reduces human operation errors, and ensures the stability of product quality in industrial production; and (3) small reaction volume, high heat exchange efficiency, and reduced by product formation at the same time, meeting the requirements of green chemical industry. This continuous flow chemistry method not only solves the mass and heat transfer bottlenecks in the scale-up of batch reactions, but also can flexibly meet different production capacity requirements by modularly expanding the number and length of reactor channels. In addition, it has strong process closure, can effectively control the introduction of impurities, reduce the cost of subsequent separation and purification, and provide an efficient and stable synthesis route for the industrial application of catalysts. Similarly, Wu et al. [124] developed a simple, fast, and solvent free microwave pyrolysis method to synthesize ultra small (3.5 nm) Ru-Mo_2C@carbon nanotube (CNT) catalysts with heterogeneous structures and strong metal support interactions in one step. This method can significantly shorten reaction time and reduce energy consumption (Fig. 7(d)).

7 Future research directions and breakthrough paths

7.1 Innovation of precise synthesis methods

Develop intelligent synthesis strategies combining ALD and machine learning. Optimize reaction parameters through algorithms to achieve atomic level precise control. For example, use high throughput screening platforms to quickly evaluate the catalytic performance of different support and metal combinations, accelerating the development of new catalysts.

Yet, current precise synthesis technologies (such as atomic layer deposition, electrochemical atomic exfoliation) have core limitations. First, the atomic scale arrangements achieved in laboratories tend to destabilize in practical applications, resulting in a compatibility contradiction with the dynamic industrial reaction environments (such as temperature fluctuations, impurity interference). Second, the optimization of synthesis parameters relies on the traditional trial and error method, leading to long development cycles and high costs. Third, artificial intelligence is difficult to integrate the multidimensional information of synthesis, characterization, and performance. Therefore, the breakthrough path to achieve the unity of precision and efficiency must center on an AI driven closed loop synthesis system. Build a multidimensional integrated dataset that covers catalyst element composition, synthesis parameters (such as pulse time of atomic layer deposition precursors, electrochemical potential), *in situ* characterization data (such as dynamic changes of atomic arrangement), and catalytic performance, so as to break the data fragmentation. Adopt transfer learning algorithms, use a small amount of noble metal catalyst data to train the basic model, and then transfer it to non-noble metal systems. Develop a real-time feedback control module, input the atomic arrangement deviations captured by *in situ* characterization into the AI model, and dynamically adjust the synthesis parameters (such as microwave power, ball milling speed).

On this basis, to break through the semi-automation limitations of traditional intelligent synthesis, a closed loop autonomous research and development system can be further introduced to realize the full process automation of catalyst discovery and optimization. This system integrates high throughput experimental platforms, real-time characterization modules, and intelligent decision-making algorithms, and can independently complete the closed loop cycle of synthesis parameter design, sample preparation, performance testing, data analysis and strategy iteration. Through algorithms to predict the element combinations and structural parameters of potential high efficiency catalysts, automated equipment completes atomic scale precise synthesis. Then, reinforcement learning is used to continuously optimize the synthesis strategy, shortening the catalyst development cycle from several years to several weeks.

In addition, the shrinkage induced self-assembly strategy has also been used to prepare a series of complexes with single crystal structures [125]. By adjusting the ratio of metal ions to other components, new topological structures with different stacking modes can be obtained, showing structural diversity and high tunability. This work not only provides an effective method for constructing lanthanide-mechanically interlocked molecules (MIMs) systems with high stability and high functionality but also lays a theoretical and practical foundation for the predictable design and precise regulation of MIMs structures in the future. These methods offer new ideas and tools for precisely controlling the distribution and arrangement of atoms on catalyst surfaces.

7.2 Rational design of active sites

Combine DFT and experimental characterization to reveal the structure–activity relationship between the coordination environment of surface atoms and catalytic performance [126, 127]. Regulate the electronic structure of the metal–support interface, optimize reactant adsorption and intermediate conversion paths, and achieve high-selectivity catalysis.

Researchers also use defect engineering to regulate the active sites of catalysts. For example, Xie and co-workers [128] created phosphorus vacancies (P-vacancies) on Rh_2P nanowires, breaking the atomic uniformity of the originally thermodynamically stable P-terminated surface. This exposes subsurface Rh atoms as exclusive H adsorption sites, while surrounding P sites adsorb OH^- to synergistically promote the reaction (Fig. 7(c)). The Rh_2P nanowires after this defect engineering achieve a mass activity 14.3 times that of commercial Pt/C and excellent CO tolerance.

Yet, the current design of active sites faces multiple bottlenecks. First, there is a lack of quantitative prediction ability. Although DFT calculations can simulate the electronic structure of single active sites, they cannot balance the synergistic effects of multiple sites and structural evolution under dynamic reaction environments, and the computational cost increases exponentially with the complexity of the system. Second, there is a lack of systematic AI assisted design methods for regulating electronic states, such as spin configurations. Third, traditional inorganic catalytic active sites are difficult to adapt to the structural requirements of different intermediates in the reaction.

Therefore, it is necessary to improve the level of rational design. (1) Develop machine learning potential energy surface models to increase the calculation speed of electronic structure for multi atomic sites (such as diatomic sites, heterotrimers) by 1000 times, while ensuring the accuracy error is less than 5%. (2) Use graph neural networks to predict the synergistic strength of active sites. The input features include atomic coordination environment, bond length, charge distribution, and others, and the output key parameters include intermediate adsorption energy, reaction energy barrier, and others, so as to precisely design multi-site structures with both high activity and selectivity. (3) Construct inorganic catalytic active sites with biomimetic recognition and adaptive regulation functions. By precisely regulating the coordination environment and spatial configuration of active centers, it is possible to simulate the specific adsorption of enzymes to substrates. Use dynamic coating layers and flexible supports to realize reversible conformational changes of active sites, adapting to the needs of different intermediates. (4) Use AI analysis to track the coordination environment and spin state changes of active sites in real-time during the reaction process, feeding back to model optimization.

In addition to the above design paths, the introduction of the active center design concept of precise recognition and dynamic regulation in biocatalysis opens up a new direction for the rational design of active sites. The active sites in enzyme catalysis can specifically bind to substrates. By precisely regulating the coordination environment and spatial configuration of the active center, it simulates the specific adsorption of substrates by enzymes. At the same time, dynamic coating layers and flexible supports are

used to realize the reversible changes of the conformation of active sites, adapting to the structural requirements of different intermediates in the catalytic reaction.

In addition, efficient catalytic reactions can be achieved by designing ordered single atom or dual-atom sites. For example, one-dimensional single atom arrays and axial dual-atom sites show excellent performance in oxygen reduction and CO_2 electroreduction reactions [129]. These research results provide a theoretical basis and experimental evidence for the design of efficient active sites.

7.3 Combination of advanced characterization technologies

Develop multi-modal *in situ* characterization technologies, such as the combination of *in situ* electron microscopy and *in situ* Raman/infrared spectroscopy, to realize real-time dynamic tracking of catalyst structure, electronic state, and reaction intermediates. Develop fast X-ray imaging technology based on XAFS to improve spatiotemporal resolution. In addition, researchers are developing more advanced calculation methods and tools, such as machine learning and artificial intelligence technologies, to analyze and predict catalyst performance and guide catalyst design. These methods can mine patterns from a large amount of experimental data, predict catalyst performance, and accelerate the development and optimization of catalysts.

Existing characterization technologies, especially *in situ* characterization, have obvious limitations. First, the time resolution of *in situ* transmission electron microscopy is at the second scale, which cannot capture instantaneous processes, such as femtosecond scale atomic migration and chemical bond breaking. Second, it cannot distinguish the dynamic differences between surface atoms and bulk atoms, active sites, and inert sites. Third, massive *in situ* characterization data, such as transmission electron microscopy image sequences and spectral curves rely on manual analysis, which can easily miss key dynamic information. Fourth, it cannot actively manipulate the catalytic reaction paths.

Therefore, it is necessary to achieve the following technological leaps. Develop cross scale *in situ* characterization technologies, integrate femtosecond laser spectroscopy and ultrafast electron microscopy, explore the observation and manipulation technologies of catalytic reactions at ultrafast time scales femtosecond scale, which can realize the leap from passive recording to active regulation. Construct AI assisted data analysis, extract parameters, such as surface atomic reconstruction rate and defect formation probability, deconvolute *in situ* Raman spectra, distinguish characteristic peaks of different reaction intermediates, and realize real-time analysis of intermediate conversion paths. Develop correlation models, integrate dynamic structure data analyzed by AI, such as changes in atomic coordination numbers and bond length fluctuations, with catalytic performance data, and establish quantitative structure activity relationships. Realize active manipulation of catalytic reactions, selectively activate specific reaction channels through precise regulation, and break through the limitations of thermodynamic equilibrium.

In addition, researchers are developing more advanced calculation methods and tools, such as machine learning and artificial intelligence technologies, for analyzing and predicting catalyst performance and guiding catalyst design. These methods can mine the underlying rules from a large amount of experimental data, predict catalyst performance, and accelerate the development and optimization of catalysts.

7.4 Construction of sustainable catalytic systems

Existing sustainable catalytic systems are still affected by cost and environmental factors, lack precise and optimized recovery methods, the application of AI technology in full process optimization is still insufficient, and traditional non noble metal alternatives fail to balance activity, stability, and sustainability.

To solve this problem, researchers have developed various strategies to achieve deep coupling between sustainability and efficiency.

Establish a database covering links, such as catalyst synthesis (raw material consumption, energy consumption), reaction (activity, stability), and recovery (separation efficiency, energy consumption); balance the catalytic activity, cost and environmental impact of the synthesized catalysts; combine *in situ* infrared spectroscopy with AI monitoring to detect deactivation signals, such as catalyst dissolution and carbon deposition during the reaction process in real-time, and extend the service life of the catalysts.

In addition to traditional sustainable strategies, such as non-noble metal substitution and catalyst recovery, the integration of synthetic biology and nano catalysis technologies to construct bioinorganic hybrid catalytic systems can achieve the deep coupling of sustainability and catalytic efficiency. For examples, Escherichia coli and cyanobacteria are engineered to express specific functional peptides or enzyme molecules on their surfaces. Then, through biomineralization, inorganic nanocatalysts are precisely attached to the surface of microorganisms, forming a hybrid system with both biological specificity and high inorganic catalytic efficiency [130]. This system can use the metabolic processes of microorganisms to provide reaction substrates, such as fixing CO_2 through photosynthesis, and achieve high efficiency conversion through inorganic catalytic sites. At the same times, it improves the catalytic stability with the self-repair ability of microorganisms.

Explore non-noble metal alternatives, such as transition metal alloys or SACs, and optimize their preparation processes to reduce costs. At the same time, design recyclable catalyst recovery processes to reduce resource waste. In addition, low cost and ultra-low dosage of noble metals provide an alternative strategy for hydrogen-related applications, and offer new ideas for the design of near surface lattice engineering at the atomic precision level for future high-performance and low cost electrocatalysts. These research results provide new ideas and methods for constructing sustainable catalytic systems.

8 Conclusions

The surface atomic engineering of metal nanocatalysts involves multiple aspects, including synthesis, structure, characterization, and application. It requires interdisciplinary collaborative innovation to break through existing bottlenecks. Combine atomic level surface processing technologies, such as defect engineering, interface regulation, and dynamic encapsulation strategies, to enhance the structural stability of catalysts in real reaction environments. Simultaneously develop low-cost and large-scale synthesis methods suitable for industrial needs, optimize process parameters through intelligent algorithms, and integrate advanced *in situ* characterization with theoretical calculations. Achieve full-

chain breakthroughs from molecular-level mechanism insight to macro-performance optimization, and ultimately promote the practical application of high-performance metal nanocatalysts in energy conversion and chemical production. Through these studies, the activity, selectivity, and stability of catalysts can be further improved, costs can be reduced, and the wide application of metal nanocatalysts in fields, such as energy conversion, environmental protection, and chemical production can be promoted. This will provide technical support for achieving the dual carbon goal and sustainable development.

Data availability

Not applicable.

Acknowledgements

This work was supported by the National Natural Science Foundation of China (No. 52272222), Taishan Scholar Young Talent Program (Nos. tsqn201909114 and tsqn201909123), and University Youth Innovation Team of Shandong Province (No. 202201010318).

Declaration of competing interest

All the contributing authors report no conflict of interests in this work. Author Lei Wang is the editorial board member of this journal, but he is not involved in the peer-review or decision of this article.

Author contribution statement

L. W. and J. P. L. supervised the review writing process. J. P. L. conceived the theme and framework of the review. Y. Y. S. designed the review's structural content, collected most of the literature materials, and performed data analysis. Z. J. S. provided technical expertise in relevant fields and assisted in revising the review. All authors participated in the review discussions and examined and revised the final manuscript. All the authors have approved the final manuscript.

Use of AI statement

During the preparation of this work, the author utilized artificial intelligence (AI) for foundational support tasks including refining specialized terminology and proofreading Chinese and English grammar. After using this tool/service, the authors reviewed and edited the content as needed and take full responsibility for the content of the publication.

References

[1] Xing, F.; Fu, Q.; Xing, F.; Zhao, J.; Long, H. Y.; Liu, T.; Li, X. F. Bismuth single atoms regulated graphite felt electrode boosting high power density vanadium flow batteries. *J. Am. Chem. Soc.* **2024**, *146*, 26024–26033.

[2] Xia, Q.; Gong, S. H.; Wu, J.; Zhai, Y. J.; Li, W. S.; Zhou, Y. Y.; Zhang, X. Electrochemical upgrading plastic to organosulfurs through Fe–N_3 single atom catalyst under ambient conditions. *Angew. Chem., Int. Ed.* **2025**, *64*, e202507901.

[3] Wang, X. X.; Winter, L. R.; Wu, X. H.; Fan, Y. Z.; Zhao, Y. M.; Kim, J. H.; Elimelech, M. Intensified atomic utilization efficiency of single atom catalysts for nitrate conversion via electrified nanoporous membrane. *Sci. Adv.* **2025**, *11*, eads6943.

[4] Wei, Z. M.; Ding, Y. X.; Shi, W. L.; Zhang, F. Y.; Song, Y. X.; Cui, X.; Guo, Y.; Sun, L. C.; Jiang, Q. K.; Zhang, B. B. Lanthanum-assisted lattice anchoring of iridium in Co_3O_4 for efficient oxygen evolution reaction in low-iridium water electrolysis. *Nat. Commun.* **2025**, *16*, 8145.

[5] Zhang, D.; Zhao, H.; Huang, B. L.; Li, B.; Li, H. D.; Han, Y.; Wang, Z. C.; Wu, X. K.; Pan, Y.; Sun, Y. J. et al. Advanced ultrathin RuPdM (M = Ni, Co, Fe) nanosheets electrocatalyst boosts hydrogen evolution. *ACS Cent. Sci.* **2019**, *5*, 1991–1997.

[6] Lv, Z.; Zhou, S. L.; Zhao, L.; Liu, Z. Y.; Liu, J. X.; Xu, W. X.; Wang, L.; Lai, J. P. Coactivation of multiphase reactants for the electrosynthesis of urea. *Adv. Energy Mater.* **2023**, *13*, 2300946.

[7] Shi, Y.; Song, L. M.; Liu, Y.; Wang, T. T.; Li, C. X.; Lai, J. P.; Wang, L. Dual cocatalytic sites synergize NiFe layered double hydroxide to boost oxygen evolution reaction in anion exchange membrane water electrolyzer. *Adv. Energy Mater.* **2024**, *14*, 2402046.

[8] Menezes, P. W.; Panda, C.; Garai, S.; Walter, C.; Guiet, A.; Driess, M. Structurally ordered intermetallic cobalt stannide nanocrystals for high-performance electrocatalytic overall water-splitting. *Angew. Chem., Int. Ed.* **2018**, *57*, 15237–15242.

[9] Wang, Y. F.; Sun, D.; Chowdhury, T.; Wagner, J. S.; Kempa, T. J.; Hall, A. S. Rapid room-temperature synthesis of a metastable ordered intermetallic electrocatalyst. *J. Am. Chem. Soc.* **2019**, *141*, 2342–2347.

[10] Guan, J. Y.; Yang, S. X.; Liu, T. T.; Yu, Y. H.; Niu, J.; Zhang, Z. P.; Wang, F. Intermetallic FePt@PtBi core–shell nanoparticles for oxygen reduction electrocatalysis. *Angew. Chem., Int. Ed.* **2021**, *60*, 21899–21904.

[11] Ai, X.; Zou, X.; Chen, H.; Su, Y. T.; Feng, X. L.; Li, Q. J.; Liu, Y. P.; Zhang, Y.; Zou, X. X. Transition-metal–boron intermetallics with strong interatomic d–sp orbital hybridization for high-performance electrocatalysis. *Angew. Chem., Int. Ed.* **2020**, *59*, 3961–3965.

[12] Yu, W. H.; Zhang, Y. Y.; Qin, Y. N.; Zhang, D.; Liu, K.; Bagliuk, G. A.; Lai, J. P.; Wang, L. High-density frustrated lewis pair for high-performance hydrogen evolution. *Adv. Energy Mater.* **2023**, *13*, 2203136.

[13] Li, H. D.; Lai, J. P.; Li, Z. J.; Wang, L. Multi-sites electrocatalysis in high-entropy alloys. *Adv. Funct. Mater.* **2021**, *31*, 2106715.

[14] Zhang, D.; Zhao, H.; Wu, X. K.; Deng, Y.; Wang, Z. C.; Han, Y.; Li, H. D.; Shi, Y.; Chen, X. L.; Li, S. X. et al. Multi-site electrocatalysts boost pH-universal nitrogen reduction by high-entropy alloys. *Adv. Funct. Mater.* **2021**, *31*, 2006939.

[15] Liu, P. F.; Zhang, X.; Fei, J. W.; Shi, Y.; Zhu, J. W.; Zhang, D.; Zhao, L.; Wang, L.; Lai, J. P. Frank partial dislocations in coplanar Ir/C ultrathin aanosheets boost hydrogen evolution reaction. *Adv. Mater.* **2024**, *36*, 2310591.

[16] Yan, D. F.; Xia, C. F.; Zhang, W. J.; Hu, Q.; He, C. X.; Xia, B. Y.; Wang, S. Y. Cation defect engineering of transition metal electrocatalysts for oxygen evolution reaction. *Adv. Energy Mater.* **2022**, *12*, 2202317.

[17] Guo, L. L.; Chi, J. Q.; Cui, T.; Zhu, J. W.; Xia, Y. N.; Guo, H. L.; Lai, J. P.; Wang, L. Phosphorus defect mediated electron redistribution to boost anion exchange membrane-based alkaline seawater electrolysis. *Adv. Energy Mater.* **2024**, *14*, 2400975.

[18] Wang, X. X.; Li, S. Y.; Yuan, Z.; Sun, Y. F.; Tang, Z.; Gao, X. Y.; Zhang, H. Y.; Li, J. X.; Wang, S. Y.; Yang, D. C. et al. Optimizing electrocatalytic nitrogen reduction via interfacial electric field modulation: Elevating *d*-band center in WS_2–WO_3 for enhanced intermediate adsorption. *Angew. Chem., Int. Ed.* **2023**, *62*, e202303794.

[19] Yu, Y. D.; Han, J. N.; Li, H. R.; Diao, H. Y.; Shi, Y.; Jin, G. Z.; Li, H. D.; Bagliuk, G. A.; Wang, L.; Lai, J. P. CuPt alloy enabling the tandem catalysis for reduction of HCOOH and NO^{3-} to urea at high current density. *Adv. Mater.* **2025**, *37*, 2419738.

[20] Li, Y. F.; Wang, H. L.; Chen, C.; Xie, X. S.; Yang, Y.; Tan, X. H.; Jiang, K. R.; Chen, N.; Zhang, H.; Li, Z. Ten thousand hour stable zinc–air batteries via Fe and W dual atom sites. *Nat. Commun.* **2025**, *16*, 8085.

[21] Liu, K. Y.; Shen, H.; Sun, Z. Y.; Zhou, Q.; Liu, G. Q.; Sun, Z. T.; Chen, W. X.; Gao, X.; Chen, P. W. Transient pulsed discharge preparation of graphene aerogel supports asymmetric Cu cluster catalysts promote CO_2 electroreduction. *Nat. Commun.* **2025**, *16*, 1203.

[22] Li, K.; Zhang, S.; Zhu, K. L.; Cui, L. P.; Yang, L.; Chen, J. J. Revealing the electrocatalytic self-assembly route from building blocks into giant Mo-blue clusters. *J. Am. Chem. Soc.* **2023**, *145*, 24889–24896.

[23] Sun, L. B.; Dai, C. C.; Wang, T. J.; Jin, X. D.; Xu, Z. J.; Wang, X. Modulating the electronic structure of cobalt in molecular catalysts via coordination environment regulation for highly efficient heterogeneous nitrate reduction. *Angew. Chem., Int. Ed.* **2024**, *63*, e202320027.

[24] Yu, Y. D.; Lv, Z.; Liu, Z. Y.; Sun, Y. Y.; Wei, Y. Y.; Ji, X.; Li, Y. Y.; Li, H. D.; Wang, L.; Lai, J. P. Activation of Ga liquid catalyst with continuously exposed active sites for electrocatalytic C–N coupling. *Angew. Chem., Int. Ed.* **2024**, *63*, e202402236.

[25] Li, H. D.; Sun, M. Z.; Pan, Y.; Xiong, J.; Du, H. Y.; Yu, Y. D.; Feng, S. H.; Li, Z. J.; Lai, J. P.; Huang, B. L. et al. The self-complementary effect through strong orbital coupling in ultrathin high-entropy alloy nanowires boosting pH-universal multifunctional electrocatalysis. *Appl. Catal. B: Environ.* **2022**, *312*, 121431.

[26] Zhou, J.; Wen, M.; Huang, R.; Wu, Q. S.; Luo, Y. X.; Tian, Y. K.; Wei, G. F.; Fu, Y. Q. Regulating active hydrogen adsorbed on grain boundary defects of nano-nickel for boosting ammonia electrosynthesis from nitrate. *Energy Environ. Sci.* **2023**, *16*, 2611–2620.

[27] Zhang, D.; Shi, Y.; Chen, X. L.; Lai, J. P.; Huang, B. L.; Wang, L. High-entropy alloy metallene for highly efficient overall water splitting in acidic media. *Chin. J. Catal.* **2023**, *45*, 174–183.

[28] Zhou, S. L.; Shi, Y.; Dai, Y.; Zhan, T. R.; Lai, J. P.; Wang, L. Continuous-flow electrosynthesis of urea and oxalic acid by CO_2-nitrate reduction and glycerol oxidation. *Chin. J. Catal.* **2024**, *63*, 270–281.

[29] Yu, Y. D.; Sun, Y. Y.; Han, J. N.; Guan, Y. J.; Li, H. D.; Wang, L.; Lai, J. P. Achieving efficient urea electrosynthesis through improving the coverage of A crucial intermediate across A broad range of nitrate concentrations. *Energy Environ. Sci.* **2024**, *17*, 5183–5190.

[30] Xu, J.; Xue, X. X.; Shao, G. L.; Jing, C. F.; Dai, S.; He, K.; Jia, P. P.; Wang, S.; Yuan, Y. F.; Luo, J. et al. Atomic level polarization in electric fields of defects for electrocatalysis. *Nat. Commun.* **2023**, *14*, 7849.

[31] Xu, H. B.; Zheng, D. J.; Wang, S.; Zheng, E. Y.; Zhang, Y. L.; Liu, T. C.; Liu, J. X.; Menga, D.; Kim, J.; Fang, J. H. et al. Stable metal–organic electrocatalysts for anion-exchange membrane water electrolyzers by defect engineering. *J. Am. Chem. Soc.* **2025**, *147*, 29838–29851.

[32] Wu, L. Y.; Wu, Q. L.; Han, Y.; Zhang, D. D.; Zhang, R. R.; Song, N.; Fang, Y. Q.; Liu, H. D.; Wang, M. Y.; Chen, J. et al. Constructing asymmetric defects pairs in electrocatalysts for efficient glycerol oxidation. *J. Am. Chem. Soc.* **2025**, *147*, 18033–18043.

[33] Zhao, L.; Lv, Z.; Shi, Y.; Zhou, S. L.; Liu, Y.; Han, J. N.; Zhang, Q.; Lai, J. P.; Wang, L. Simultaneous generation of furfuryl alcohol, formate, and H_2 by co-electrolysis of furfuryl and HCHO over bifunctional CuAg bimetallic electrocatalysts at ultra-low voltage. *Energy Environ. Sci.* **2024**, *17*, 770–779.

[34] Zhao, L.; Lv, Z.; Shi, Y.; Zhou, S. L.; Liu, Y.; Han, J. N.; Zhang, Q.; Lai, J. P.; Wang, L. Correction: Simultaneous generation of furfuryl alcohol, formate, and H_2 by Co-electrolysis of furfural and HCHO over bifunctional CuAg bimetallic electrocatalysts at ultra-low voltage. *Energy Environ. Sci.* **2024**, *17*, 1291–1291.

[35] Zhang, D.; Shi, Y.; Zhao, H.; Qi, W. J.; Chen, X. L.; Zhan, T. R.; Li, S. X.; Yang, B.; Sun, M. Z.; Lai, J. P. et al. The facile oil-phase synthesis of a multi-site synergistic high-entropy alloy to promote the alkaline hydrogen evolution reaction. *J. Mater. Chem. A* **2021**, *9*, 889–893.

[36] Sun, Y. T.; Lu, G. G.; Wang, Z. Q.; Li, X. H.; Li, Y. H.; Sui, N. L. D.; Fan, W. J.; Wang, A.; Yuan, B.; Wang, J. J. et al. Size effect of surface defects dictates reactivity for nitrogen electrofixation. *Angew. Chem., Int. Ed.* **2025**, *64*, e202425112.

[37] Shen, S. J.; Li, Q.; Zhang, H. H.; Yang, D.; Gong, J. J.; Gu, L.; Gao, T.; Zhong, W. W. Negative-valent platinum stabilized by Pt–Ni electron bridges on oxygen-deficient NiFe-LDH for enhanced electrocatalytic hydrogen evolution. *Adv. Mater.* **2025**, *37*, 2500595.

[38] Maiti, S.; Maiti, K.; Curnan, M. T.; Kim, K.; Noh, K. J.; Han, J. W. Engineering electrocatalyst nanosurfaces to enrich the activity by inducing lattice strain. *Energy Environ. Sci.* **2021**, *14*, 3717–3756.

[39] Liu, Y.; Bui, H. T. D.; Jadhav, A. R.; Yang, T.; Saqlain, S.; Luo, Y. G.; Yu, J. M.; Kumar, A.; Wang, H. D.; Wang, L. L. et al. Revealing the synergy of cation and anion vacancies on improving overall water splitting kinetics. *Adv. Funct. Mater.* **2021**, *31*, 2010718.

[40] Shahid, U. B.; Kwon, Y.; Yuan, Y.; Gu, S.; Shao, M. H. High-performance ammonia electrosynthesis from nitrate in a NaOH–KOH–H_2O ternary electrolyte. *Angew. Chem., Int. Ed.* **2024**, *63*, e202403633.

[41] Qi, M. H.; Du, X. B. W.; Shi, X. Y.; Wang, S. W.; Lu, B.; Chen, J. D.; Mao, S. J.; Zhang, H.; Wang, Y. Single atom Ru-triggered lattice oxygen redox mechanism for enhanced acidic water oxidation. *J. Am. Chem. Soc.* **2025**, *147*, 18295–18306.

[42] Lan, J.; Wang, Z.; Kao, C. W.; Lu, Y. R.; Xie, F.; Tan, Y. W. Isolating Cu–Zn active-sites in ordered intermetallics to enhance nitrite-to-ammonia electroreduction. *Nat. Commun.* **2024**, *15*, 10173.

[43] Mu, W. L.; Li, L. Y.; Cong, X. Z.; Chen, X. Y.; Xia, P. K.; Liu, Q. Y.; Wang, L. K.; Yan, J.; Liu, C. Hierarchical assembly of high-nuclearity copper(I) alkynide nanoclusters: Highly effective CO_2 electroreduction catalyst toward hydrocarbons. *J. Am. Chem. Soc.* **2024**, *146*, 28131–28140.

[44] Huang, Q. P.; Xia, G. J.; Huang, B.; Xie, D. L.; Wang, J.; Wen, D.; Lin, D. M.; Xu, C. G.; Gao, L.; Wu, Z. D. et al. Activating lattice oxygen by A defect-engineered Fe_2O_3–CeO_2 nano-heterojunction for efficient electrochemical water oxidation. *Energy Environ. Sci.* **2024**, *17*, 5260–5272.

[45] Lu, K.; Xia, F.; Li, B. M.; Liu, Y. Z.; Abdul Razak, I. B.; Gao, S. Y.; Kaelin, J.; Brown, D. E.; Cheng, Y. W. Synergistic multisites $Fe_2Mo_6S_8$ electrocatalysts for ambient nitrogen conversion to ammonia. *ACS Nano* **2021**, *15*, 16887–16895.

[46] Liu, M. D.; Zhang, S.; Chen, M.; Wu, L. M. Boosting electrochemical nitrogen reduction performance through water-in-salt electrolyte. *Appl. Catal. B: Environ.* **2022**, *319*, 121925.

[47] Liang, S. Z.; Teng, X.; Xu, H.; Chen, L. S.; Shi, J. L. H* species regulation by Mn–$Co(OH)_2$ for efficient nitrate electro-reduction in neutral solution. *Angew. Chem., Int. Ed.* **2024**, *63*, e202400206.

[48] Guo, Y. X.; Stroka, J. R.; Kandemir, B.; Dickerson, C. E.; Bren, K. L. Cobalt metallopeptide electrocatalyst for the selective reduction of nitrite to ammonium. *J. Am. Chem. Soc.* **2018**, *140*, 16888–16892.

[49] Duca, M.; Figueiredo, M. C.; Climent, V.; Rodriguez, P.; Feliu, J. M.; Koper, M. T. M. Selective catalytic reduction at quasi-perfect Pt (100) domains: A universal low-temperature pathway from nitrite to N_2. *J. Am. Chem. Soc.* **2011**, *133*, 10928–10939.

[50] Duca, M.; Cucarella, M. O.; Rodriguez, P.; Koper, M. T. M. Direct reduction of nitrite to N_2 on a Pt (100) electrode in alkaline media. *J. Am. Chem. Soc.* **2010**, *132*, 18042–18044.

[51] Cheng, Y.; Xu, X. N.; Wang, M. F.; Deng, C. W.; Sun, Y.; Yan, C. L.; Qian, T. Interfacial proton supply/filtration regulates the dynamics of electrocatalytic nitrogen reduction reaction: A perspective. *Adv. Funct. Mater.* **2023**, *33*, 2302332.

[52] Kessels, E.; Devi, A.; Park, J. S.; Ritala, M.; Yanguas-Gil, A.;

Wiemer, C. Atomic layer deposition. *Nat. Rev. Methods Primers* **2025**, *5*, 66.

[53] Kazuma, E.; Jung, J.; Ueba, H.; Trenary, M.; Kim, Y. Real-space and real-time observation of a plasmon-induced chemical reaction of a single molecule. *Science* **2018**, *360*, 521–526.

[54] Ma, Y.; Yang, Q.; Qi, J.; Zhang, Y.; Gao, Y. L.; Zeng, Y.; Jiang, N.; Sun, Y.; Qu, K. Q.; Fang, W. H. et al. Surface atom knockout for the active site exposure of alloy catalyst. *Proc. Natl. Acad. Sci. USA* **2024**, *121*, e2319525121.

[55] Zhao, L.; Tao, Z. T.; You, M. S.; Xiao, H. W.; Wang, S. J.; Ma, W. J.; Huang, Y. L.; He, B. B.; Chen, Q. Partial exsolution enables superior bifunctionality of Ir@$SrIrO_3$ for acidic overall water splitting. *Adv. Sci.* **2024**, *11*, 2309750.

[56] Głowniak, S.; Szczęśniak, B.; Choma, J.; Jaroniec, M. Advances in microwave synthesis of nanoporous materials. *Adv. Mater.* **2021**, *33*, 2103477.

[57] Wu, Z. X.; Yang, P. F.; Li, Q. C.; Xiao, W. P.; Li, Z. J.; Xu, G. R.; Liu, F. S.; Jia, B. H.; Ma, T. Y.; Feng, S. H. et al. Microwave synthesis of Pt clusters on black TiO_2 with abundant oxygen vacancies for efficient acidic electrocatalytic hydrogen evolution. *Angew. Chem., Int. Ed.* **2023**, *62*, e202300406.

[58] Gan, T.; Liu, Y. F.; He, Q.; Zhang, H.; He, X. H.; Ji, H. B. Facile synthesis of kilogram-scale Co-alloyed Pt single atom catalysts via ball milling for hydrodeoxygenation of 5-hydroxymethylfurfural. *ACS Sustain. Chem. Eng.* **2020**, *8*, 8692–8699.

[59] Zhao, J.; Han, X. C.; Li, J. X.; Han, Z. Y.; Zhao, X. X. Atomically dispersed catalytic platinum anti-substitutions in molybdenum ditelluride. *J. Am. Chem. Soc.* **2025**, *147*, 9825–9835.

[60] Speight, I. R.; Ardila-Fierro, K. J.; Hernández, J. G.; Emmerling, F.; Michalchuk, A. A. L.; García, F.; Colacino, E.; Mack, J. Ball milling for mechanochemical reactions. *Nat. Rev. Methods Primers* **2025**, *5*, 29.

[61] Kwak, I. C.; Kim, J.; Moon, J. W.; Kim, S.; Park, J. Y.; Song, O.; Mazánek, V.; Sofer, Z.; Jo, H.; Park, S. Y. et al. Orthogonal photopatterning of two-dimensional percolated network films for wafer-scale heterostructures. *Nat. Electron.* **2025**, *8*, 235–243.

[62] Reda, A. T.; Park, Y. T. Sustainable synthesis of functional nanomaterials: Renewable resources, energy-efficient methods, environmental impact and circular economy approaches. *Chem. Eng. J.* **2025**, *516*, 163894.

[63] Li, S. Z.; Luo, X.; Wang, Y. S.; Wang, C. W.; Zhang, G. Z.; Xiang, H. X.; Yan, Y.; Ke, X. X.; Lu, Y.; Yao, C. H. et al. Strong oxide-support interaction induced thermal stabilization of Pt single atoms for durable catalytic CO oxidation. *Angew. Chem., Int. Ed.* **2025**, *64*, e202504551.

[64] Wang, X. L.; Fu, N. H.; Liu, J. C.; Yu, K.; Li, Z.; Xu, Z. F.; Liang, X.; Zhu, P.; Ye, C. L.; Zhou, A. W. et al. Atomic replacement of PtNi nanoalloys within Zn-ZIF-8 for the fabrication of a multisite CO_2 reduction electrocatalyst. *J. Am. Chem. Soc.* **2022**, *144*, 23223–23229.

[65] Chen, X. W.; Wang, M. L.; He, Y. R.; Peng, M.; Diao, J. Y.; Xiao, D. Q.; Wang, N.; Cai, X. B.; Liu, H. Y.; Ma, D. A highly efficient and regenerable Ir_1–Cu_1 dual-atom catalyst for low-temperature alkane dehydrogenation. *Nat. Catal.* **2025**, *8*, 436–447.

[66] Fan, R. Y.; Liu, H. J.; Ren, J. K.; Li, Y. C.; Nan, J.; Zhou, Y. L.; Liu, C. Y.; Chai, Y. M.; Dong, B. Ligand-confinement-induced catalyst–support interface interactions in Co_3O_4-supported RuO_2 for long-term stable acidic oxygen evolution reaction. *ACS Sustain. Chem. Eng.* **2024**, *12*, 2313–2323.

[67] Muhuri, D.; Sarkar, M.; Duan, H. Y.; Hanson, L. A.; He, J. Polymer ligands with quaternary ammonium binding motifs on metal nanoparticles enable selective ion transport for CO_2 electroreduction. *Angew. Chem., Int. Ed.* **2025**, *137*, e202516071.

[68] Kong, X. D.; Zhu, J. C.; Xu, Z. F.; Geng, Z. G. Fundamentals and challenges of ligand modification in heterogeneous electrocatalysis. *Angew. Chem., Int. Ed.* **2025**, *64*, e202417562.

[69] Lopes, P. P.; Li, D. G.; Lv, H. F.; Wang, C.; Tripkovic, D.; Zhu, Y. S.; Schimmenti, R.; Daimon, H.; Kang, Y. J.; Snyder, J. et al. Eliminating dissolution of platinum-based electrocatalysts at the atomic scale. *Nat. Mater.* **2020**, *19*, 1207–1214.

[70] Zhu, B.; Huang, S. D.; Seo, O.; Cao, M. N.; Matsumura, D.; Gu, H. Y.; Wu, D. S. Stabilizing the unstable: Enhancing OER durability with 3d-orbital transition metal multielemental alloy nanoparticles by atomically dispersed 4d-orbital Pd for a 100-fold extended lifetime. *J. Am. Chem. Soc.* **2025**, *147*, 11250–11256.

[71] Wei, M. J.; Li, J. W.; Zhao, J. K.; Hu, S. P.; Ji, Y.; Xue, W. Q.; Dai, Y. Z.; Wang, H. Y.; Zhang, X. Y.; Hui, K. N. et al. Stabilization of oxidized cu species via CeO_x nano-islands for enhanced CO_2 reduction to C_{2+} products. *Natl. Sci. Rev.* **2025**, *12*, nwaf351.

[72] Wu, B.; Yang, H. L.; Li, L. B.; Tang, X. N.; Wu, Y. G.; Huang, B. Y.; Lützenkirchen-Hecht, D.; Qiu, M.; Yuan, K.; Chen, Y. W. Integrating PtCo intermetallic with highly graphitized carbon toward durable oxygen electroreduction in proton exchange membrane fuel cells. *Adv. Mater.* **2025**, *37*, 2500096.

[73] Wang, C. L.; Zhao, Z. Y.; Cao, W. J.; Peng, Y. J.; Song, M. W.; Wu, Y. F. A metal-free carbonaceous material for highly efficient and robust electrochemical biomass valorization. *Adv. Funct. Mater.* **2025**, *35*, 2502618.

[74] Jiang, H. M.; He, J. Y.; Zhou, S. T.; Yuan, M. W.; Lin, L.; Sun, Z. M.; Sun, G. B. Electron donor–acceptor activated anti-fenton property for the ultradurable oxygen reduction reaction. *ACS Nano* **2025**, *19*, 12161–12169.

[75] Zhao, H. H.; Xu, X.; Cui, W. Q.; Geng, L. L.; Peng, X. M.; Yang, J. R.; Shao, X. Z.; Liu, Y. B. Synchronization strategy for activity and stability in fenton-like single atom catalysis. *Adv. Mater.* **2025**, *37*, 2503217.

[76] Li, S. S.; Wang, W.; Wu, H. Z.; Wang, X. C.; Ding, S. H.; Liu, J. Y.; Zhang, X. W.; Sun, J. L.; Fu, C. H.; Zhou, M. H. Facile cascade-anchored synthesis of ultrahigh metal loading single atom for significantly improved fenton-like catalysis. *Nat. Commun.* **2025**, *16*, 8796.

[77] Peng, B. S.; Liu, Z. Y.; Sementa, L.; Jia, Q. Y.; Sun, Q.; Segre, C. U.; Liu, E. S.; Xu, M. J.; Tsai, Y. H.; Yan, X. X. et al. Embedded oxide clusters stabilize sub-2 nm pt nanoparticles for highly durable fuel cells. *Nat. Catal.* **2024**, *7*, 818–828.

[78] Tao, F.; Salmeron, M. Surface restructuring and predictive design of heterogeneous catalysts. *Science* **2024**, *386*, eadq0102.

[79] Kong, F. P.; Ren, Z. H.; Norouzi Banis, M.; Du, L.; Zhou, X.; Chen, G. Y.; Zhang, L.; Li, J. J.; Wang, S. Z.; Li, M. S. et al. Active and stable Pt–Ni alloy octahedra catalyst for oxygen reduction via near-surface atomical engineering. *ACS Catal.* **2020**, *10*, 4205–4214.

[80] Kim, J. H.; Yun, H.; Kim, C. G.; Kim, N.; Yang, Y.; Yoo, S.; Moon, D.; Kim, D.; Hong, C. S. Postsynthetic triazolate functionalization of Ni_2Cl_2BTDD: Creation of supplementary CO_2 adsorption sites and exceptional CO_2 selectivity. *J. Am. Chem. Soc.* **2025**, *147*, 37732–37740.

[81] Fan, W. P.; Zhang, Q.; Gong, X. Q.; Lou, Y.; Wang, D. Dual-stabilization strategy for inhibiting metal nanoparticle sintering over ceria surfaces. *Angew. Chem., Int. Ed.*, in press, DOI: 10.1002/anie.202518312.

[82] Wang, P.; Zheng, J.; Li, Y. Y.; Shi, Q. F.; Zhang, J.; Wan, Y.; Niu, M.; Yamauchi, Y.; Long, Y. Z. Catalyst for industrial-scale seawater electrolysis: Inhibit active metal dissolution and chlorine corrosion. *Adv. Sci.* **2025**, *12*, e14301.

[83] Townsend, W. J. V.; López-Alcalá, D.; Bird, M. A.; Jordan, J. W.; Rance, G. A.; Biskupek, J.; Kaiser, U.; Baldoví, J. J.; Walsh, D. A.; Johnson, L. R. et al. The role of carbon catalyst coatings in the electrochemical water splitting reaction. *Nat. Commun.* **2025**, *16*, 4460.

[84] Zhang, T.; Li, T.; Shen, Y.; Ma, H. X.; Wei, C. Y.; Cai, J. H.; Xu, Y.; Li, Y. Y.; Dong, X. J.; Zhang, S. C. et al. Enhanced kinetics and stability of Zn–MnO_2 batteries with a multifunctional TiO_2 coating.

Adv. Mater. **2025**, *37*, 2505082.

[85] Albertini, P. P.; Calderon Mora, J.; Guskova, M.; Rodlamul, P.; Hicks, N.; Leemans, J.; Loiudice, A.; Buonsanti, R. Active sites under electronic effect are more sensitive to microenvironment in CO_2 electroreduction. *J. Am. Chem. Soc.* **2025**, *147*, 25517–25526.

[86] Li, J. Y.; Zhu, X. T.; Xu, Z.; Ren, H. X.; Muhammad, S.; Yang, H. X.; Luo, B. Q.; Javed, M. U.; Yu, C.; Zhang, Y. H. et al. Dynamic metal-ligand coordinated self-healing polymer electrolytes for lithium-ion batteries: Correlating coordination mechanisms with electrochemical properties. *Adv. Funct. Mater.* **2025**, *35*, e10177.

[87] Cooper, C. B.; Root, S. E.; Michalek, L.; Wu, S.; Lai, J. C.; Khatib, M.; Oyakhire, S. T.; Zhao, R.; Qin, J.; Bao, Z. N. Autonomous alignment and healing in multilayer soft electronics using immiscible dynamic polymers. *Science* **2023**, *380*, 935–941.

[88] Song, S. J.; Ma, X. R.; Yang, L. Y.; Zhang, L. F.; Guo, J.; Zhao, Z.; Zhang, R. G.; Liu, J.; Song, W. Y.; Xu, C. M. Modulating propane dehydrogenation over silicalite-1-encapsulated CoO_x catalysts via surface silanol engineering for surface barrier control. *ACS Catal.* **2025**, *15*, 17958–17970.

[89] Wei, C. Y.; Liu, C.; Zhang, Z. Y.; Sun, K.; Xing, C. K.; Shi, W. J.; Li, Y. Y.; Li, J. F.; Zhang, B. Dynamic template reconstruction induced mesoporous iridium catalysts for high-current-density PEMWE. *Joule* **2025**, *9*, 102058.

[90] Guo, C.; Fan, X. Y.; Liu, M. T.; Xu, S. W.; Wei, G. X.; Chen, Z. B.; Guan, Z. K.; Xiao, Y.; Xin, H. S.; Wang, P. F. Amorphous protective layers to reshape inorganic-rich interphases for high-voltage sodium-ion batteries. *Carbon Energy*, in press, DOI: 10.1002/cey2.70037.

[91] Chen, S.; Xu, Y. Y.; Chang, X.; Pan, Y.; Sun, G. D.; Wang, X. H.; Fu, D. L.; Pei, C. L.; Zhao, Z. J.; Su, D. et al. Defective TiO_x overlayers catalyze propane dehydrogenation promoted by base metals. *Science* **2024**, *385*, 295–300.

[92] Ma, Z. Q.; Yuan, Z. H.; Xue, J.; Dong, Y. L.; Tan, X.; Jin, F. Y.; Li, X. G.; Gu, Y.; Chen, L. W.; Wang, K. et al. Recent advances in regulating metal-silica interaction for boosting heterogeneous catalytic performance. *Angew. Chem., Int. Ed.* **2025**, *64*, e202512979.

[93] Chen, Y. H.; Hao, J. T.; Zhang, K.; Li, S. D.; Han, Z. K.; Yuan, W. T.; Jiang, Y.; Zhang, Z.; Wang, Y. Oscillatory strong metal–support interaction in Pd/TiO_2 under redox conditions. *Angew. Chem., Int. Ed.* **2025**, *64*, e202504686.

[94] Song, M. X.; Song, S. J.; Hou, G.; Li, W. J.; Lyu, X. T.; Lyu, J. F.; Yang, C. H.; Feng, S. Z.; Wang, R. Y.; Zhang, B. F. et al. Zeolite-encapsulated Ir single atom catalysts toward efficient and stable propane dehydrogenation. *J. Am. Chem. Soc.*, in press, DOI: 10.1021/jacs.5c16066.

[95] Chen, L. N.; Song, Z. G.; Zhang, S. C.; Chang, C. K.; Chuang, Y. C.; Peng, X. X.; Dun, C.; Urban, J. J.; Guo, J. H.; Chen, J. L. et al. Ternary NiMo–Bi liquid alloy catalyst for efficient hydrogen production from methane pyrolysis. *Science* **2023**, *381*, 857–861.

[96] Zuraiqi, K.; Jin, Y. C.; Parker, C. J.; Meilak, J.; Meftahi, N.; Christofferson, A. J.; Russo, S. P.; Spencer, M. J. S.; Zhu, H. Y.; Wang, L. Z. et al. Unveiling metal mobility in a liquid Cu–Ga catalyst for ammonia synthesis. *Nat. Catal.* **2024**, *7*, 1044–1052.

[97] Wang, F.; Li, K.; Li, B. L.; Wang, C. X.; Li, Z.; Zhang, Y.; Shan, W. P.; Yu, Y. B.; Zhang, C. B.; Fu, Q. et al. Identification of direct anchoring sites for monoatomic dispersion of precious metals (Pt, Pd, Ag) on CeO_2 support. *Angew. Chem., Int. Ed.* **2024**, *63*, e202318492.

[98] Wang, L. X.; Wang, J.; Gao, X. P.; Chen, C.; Da, Y. L.; Wang, S. C.; Yang, J.; Wang, Z. Y.; Song, J.; Yao, T. et al. Periodic one-dimensional single atom arrays. *J. Am. Chem. Soc.* **2022**, *144*, 15999–16005.

[99] Zhou, D.; Wang, J. J.; Jian, M. Z.; Li, Y.; Jiang, Z.; Liu, S.; Zhou, Y.; Wei, J. K.; Wöll, C.; Li, W. X. et al. Fine-tuned coordination environment of Pt–Fe–Pt active site for selective heterogeneous hydrogenation of crotonaldehyde. *Chem* **2025**, *11*, 102380.

[100] Lu, X. J.; Wu, J. Z.; He, X. Y.; Li, Z. C.; Lu, Y. F.; Li, W. Q.; Li, J.; Xu, M.; Qi, Y. P.; Zhang, Q. et al. Ordered single active sites for cascade hydrogenation and hydroformylation reactions. *Nat. Catal.* **2025**, *8*, 536–547.

[101] Wang, W.; Cheng, X. Y.; Li, H. G.; Li, M. L.; Chen, L.; Yang, J.; Jiang, Y. X.; Huang, R.; Sun, S. G. A phosphorus-bridged spin trigger for oxygen reduction. *Angew. Chem., Int. Ed.*, in press, DOI: 10.1002/anie.202522880.

[102] Du, C. Y.; Ge, Z. Q.; Ouyang, L. H.; Xu, H. Y.; Ma, H. Y.; Wang, X. T.; Liu, Z. Q. Spin-matching effect triggering enhanced oxygen reduction reaction in acidic and alkaline media. *Angew. Chem., Int. Ed.* **2026**, *65*, e15517.

[103] Ge, X.; Zheng, X. Y.; Zhou, T.; Tian, L. J.; Wang, W.; Chen, J. J.; Wang, X. Z. Engineering spin state of atomic iron centers for high-performance photocatalytic nitrogen fixation. *Angew. Chem., Int. Ed.* **2025**, *64*, e202506470.

[104] Xie, F. K.; Du, Y.; Lu, M. F.; Yan, S. C.; Zou, Z. G. Thermal-stimulated spin disordering accelerates water electrolysis. *Energy Environ. Sci.* **2025**, *18*, 1972–1983.

[105] Lou, S. Y.; Wen, G. J.; Xu, S. K.; Zhao, J. W.; Wang, Y. S.; Chen, Y. Y.; Wang, Y.; Wen, N.; Xu, C.; Lin, H. X. et al. Stabilizing the high spin cobalt atoms by local magnetic asymmetry in p-block metals-doped spinel $MnCo_2O_4$ catalysts for efficient oxygen reduction. *Adv. Mater.* **2026**, *38*, e13681.

[106] Li, M.; Yang, J.; Li, S. X.; Deng, L. M.; Zhao, S.; Li, L. L.; Hung, S. F.; Xing, G. Y.; Wang, T.; Liang, Y. Y. et al. Rare-earth-induced intermediate-spin Co centers in $MnCo_2O_{4.5}$ for sustainable acidic water oxidation. *J. Am. Chem. Soc.* **2025**, *147*, 45680–45690.

[107] Zhang, P. X.; Liu, S. L.; Cai, L. B.; Jiang, J. C.; Zhao, X. Y.; Wu, X. L.; Li, B. J.; Xia, B. Y.; Liu, Y. Y. Axial phosphate coordination driven spin state change in FeN_4 site for stable oxygen reduction. *Angew. Chem., Int. Ed.*, in press, DOI: 10.1002/anie.202524529.

[108] Wang, Z. X.; Wan, J. L.; Sun, X. H.; Sun, L. C.; Chen, S. L.; Zhang, Q. F. Boosting the selectivity in oxygen electrocatalysis using chiral nanoparticles as electron-spin filters. *J. Am. Chem. Soc.* **2025**, *147*, 15767–15776.

[109] Wang, L. X.; Gao, X. P.; Wang, S. C.; Chen, C.; Song, J.; Ma, X. H.; Yao, T.; Zhou, H.; Wu, Y. E. Axial dual atomic sites confined by layer stacking for electroreduction of CO_2 to tunable syngas. *J. Am. Chem. Soc.* **2023**, *145*, 13462–13468.

[110] Li, H. D.; Han, Y.; Zhao, H.; Qi, W. J.; Zhang, D.; Yu, Y. D.; Cai, W. W.; Li, S. X.; Lai, J. P.; Huang, B. L. et al. Fast site-to-site electron transfer of high-entropy alloy nanocatalyst driving redox electrocatalysis. *Nat. Commun.* **2020**, *11*, 5437.

[111] Wu, Z. P.; Dinh, D.; Maswadeh, Y.; Caracciolo, D. T.; Zhang, H.; Li, T. Y.; Vargas, J. A.; Madiou, M.; Chen, C. L.; Kong, Z. J. et al. Interfacial reactivity-triggered oscillatory lattice strains of nanoalloys. *J. Am. Chem. Soc.* **2024**, *146*, 35264–35274.

[112] Che, F.; Gao, F. F.; Li, Q.; Ren, W.; Tang, H. H.; Zaina, G.; Zhang, X.; Yao, S.; Zhang, N.; Zhu, S. C. et al. Fractal analysis based on Gd-EOB-DTPA-enhanced MRI for prediction of vessels that encapsulate tumor clusters in patients with hepatocellular carcinoma. *Int. J. Surg.* **2025**, *111*, 4389–4399.

[113] Cusumano, D.; Dinapoli, N.; Boldrini, L.; Chiloiro, G.; Gatta, R.; Masciocchi, C.; Lenkowicz, J.; Casà, C.; Damiani, A.; Azario, L. et al. Fractal-based radiomic approach to predict complete pathological response after chemo-radiotherapy in rectal cancer. *Radiol. Med.* **2018**, *123*, 286–295.

[114] Cheng, X.; Li, Y. H.; Zheng, L. R.; Yan, Y.; Zhang, Y. F.; Chen, G.; Sun, S. R.; Zhang, J. J. Highly active, stable oxidized platinum clusters as electrocatalysts for the hydrogen evolution reaction. *Energy Environ. Sci.* **2017**, *10*, 2450–2458.

[115] Cheng, W. R.; Lu, X. F.; Luan, D. Y.; Lou, X. W. D. NiMn-based bimetal–organic framework nanosheets supported on multi-channel carbon fibers for efficient oxygen electrocatalysis. *Angew. Chem., Int. Ed.* **2020**, *59*, 18234–18239.

[116] Han, X.; Zhang, T. Y.; Chen, W. X.; Dong, B.; Meng, G.; Zheng, L. R.; Yang, C.; Sun, X. M.; Zhuang, Z. B.; Wang, D. S. et al. Oxygen reduction reaction: $Mn–N_4$ oxygen reduction electrocatalyst: *Operando* investigation of active sites and high performance in zinc–air battery (Adv. Energy Mater. 6/2021). *Adv. Energy Mater* **2021**, *11*, 2170025.

[117] Wang, X.; Wang, Y. Q.; Feng, Y. C.; Wang, D.; Wan, L. J. Insights into electrocatalysis by scanning tunnelling microscopy. *Chem. Soc. Rev.* **2021**, *50*, 5832–5849.

[118] Sun, Y. Y.; Han, Y.; Zhang, X. Y.; Cai, W. W.; Zhang, Y. Y.; Zhang, Y.; Li, Z. J.; Li, B.; Lai, J. P.; Wang, L. $TiO_{1.8}$ with lattice H for effective electrocatalytic nitrogen fixation. *Appl. Catal. B: Environ.* **2022**, *319*, 121933.

[119] Sun, Y. Y.; Yu, Y. D.; Xu, W. X.; Wu, D.; Wei, Y. Y.; Lai, J. P.; Wang, L. ·H effectively enhance electrocatalytic nitrogen fixation. *J. Colloid Interface Sci.* **2023**, *640*, 619–625.

[120] Liu, K. Y.; Sun, Z. Y.; Peng, X. J.; Liu, X. D.; Zhang, X.; Zhou, B. R.; Yu, K. D.; Chen, Z. B.; Zhou, Q.; Zhang, F. et al. Tailoring asymmetric RuCu dual-atom electrocatalyst toward ammonia synthesis from nitrate. *Nat. Commun.* **2025**, *16*, 2167.

[121] Han, G. F.; Li, F.; Rykov, A. I.; Im, Y. K.; Yu, S. Y.; Jeon, J. P.; Kim, S. J.; Zhou, W. H.; Ge, R. L.; Ao, Z. M. et al. Abrading bulk metal into single atoms. *Nat. Nanotechnol.* **2022**, *17*, 403–407.

[122] Liu, Z. J.; Jiang, Y. L.; Zhang, Z. X.; Wang, X. X.; Liu, K.; Qiao, Z.; Liu, M. X.; Zhang, S. M.; Mu, Z. R.; Zhang, Q. et al. Synthesis of noble/non-noble metal alloy nanostructures via an active-hydrogen-involved interfacial reduction strategy. *Nat. Synth.* **2023**, *2*, 119–128.

[123] Xu, J. C.; Zhai, G. Y.; Wang, G.; Yang, S. Y.; Liu, Z. Z.; Li, Z. L.; Li, J. W.; Yang, C.; Liu, C. Y.; Pan, Y. et al. Continuous flow photocatalysis boosting C–N coupling for sustainable high-efficiency formamide synthesis. *Angew. Chem., Int. Ed.* **2025**, *64*, e202515803.

[124] Wu, X. K.; Wang, Z. C.; Zhang, D.; Qin, Y. N.; Wang, M. H.; Han, Y.; Zhan, T. R.; Yang, B.; Li, S. X.; Lai, J. P. et al. Solvent-free microwave synthesis of ultra-small Ru–Mo_2C@CNT with strong metal–support interaction for industrial hydrogen evolution. *Nat. Commun.* **2021**, *12*, 4018.

[125] Zhang, X.; Sessler, J. L.; Gong, H. Y. Synergic regulation of mechanically interlocked molecules via lanthanide-contraction-based metal modulation and constituent ratios. *Sci. China Chem.* **2026**, *69*, 300–308.

[126] Yuan, Q.; Gu, Y. T.; Li, X. J.; Ding, Y. M.; Chen, H. Y.; Song, X. G.; Mu, J. L.; Li, B.; Cai, Y. T.; Zhang, Y. et al. Single-site palladium on sulfur-doped carbon for olefin alkoxycarbonylation: Performance determined by coordination environments. *Chem Catal.* **2024**, *4*, 100830.

[127] Yang, L.; Wu, Z. L.; Tian, T.; Huang, B. K.; Wang, X. H.; Zhang, Y.; Zhang, H.; He, C. S.; Xiong, Z. K.; Lai, B. Thermal-driven coordination microenvironment reconstruction in single atom catalysts unlocks ultrafast water remediation. *ACS Nano* **2025**, *19*, 26701–26714.

[128] Huang, H. P.; Liu, K.; Yang, F. L.; Cai, J. L.; Wang, S. P.; Chen, W. Z.; Wang, Q. X.; Fu, L. H.; Xie, Z. X.; Xie, S. F. Breaking surface atomic monogeneity of Rh_2P nanocatalysts by defect-derived phosphorus vacancies for efficient alkaline hydrogen oxidation. *Angew. Chem., Int. Ed.* **2023**, *62*, e202315752.

[129] Liu, L. Z.; Hu, J. C.; Ma, Z. Y.; Zhu, Z. J.; He, B.; Chen, F.; Lu, Y.; Xu, R.; Zhang, Y. H.; Ma, T. Y. et al. One-dimensional single atom arrays on ferroelectric nanosheets for enhanced CO_2 photoreduction. *Nat. Commun.* **2024**, *15*, 305.

[130] Cui, J. Y.; Sun, H. L.; Chen, R. Z.; Sun, J. H.; Mo, G. L.; Luan, G. D.; Lu, X. F. Multiple routes toward engineering efficient cyanobacterial photosynthetic biomanufacturing technologies. *Green Carbon* **2023**, *1*, 210–226.